A NEW PLATANISTOID (CETACEA, ODONTOCETI) FROM THE NYE FORMATION OF OREGON

by

Margot D. Nelson

A Thesis
Submitted to the
Graduate Faculty
of
George Mason University
in Partial Fulfillment of
The Requirements for the Degree
of
Master of Science,
Earth Systems Science

Committee:

_____	Dr. Mark D. Uhen, Thesis Director
_____	Dr. Stacey Verardo, Committee Member
_____	Dr. Geoffrey Gilleaudeau, Committee Member
_____	Dr. Dieter Pfoser, Department Chairperson
_____	Dr. Donna M. Fox, Associate Dean, Office of Student Affairs & Special Programs, College of Science
_____	Dr. Peggy Agouris, Dean, College of Science
Date: _____	Spring Semester 2019 George Mason University Fairfax, VA

A New Platanistoid (Cetacea, Odontoceti) from the Nye Formation of Oregon

A Thesis submitted in partial fulfillment of the requirements for the degree of Master of Science, at George Mason University

by

Margot D. Nelson
Bachelor of Science
University of Washington, 2015

Director: Mark D. Uhen, Associate Professor
Department of Atmospheric, Oceanic, and Earth Sciences

Spring Semester 2019
George Mason University
Fairfax, VA

DEDICATION

This is dedicated to my family: my parents, sister, horses, and pets, who have showered me with unconditional love.

ACKNOWLEDGEMENTS

I would like to thank my advisor, Dr. Mark D. Uhen, as well as my thesis committee members, Dr. Stacey Verardo and Dr. Geoff Gilleaudeau. I would also like to thank Douglas Emlong, who collected the specimen described in my thesis, and Matthew Eberle, who prepared the specimen. I thank several colleagues: Dr. Nick D. Pyenson, curator of fossil marine mammals at the Smithsonian National Museum of Natural History; Dave Bohaska, collections manager at the Smithsonian; Dr. Olivier Lambert, Royal Belgian Institute of Natural Sciences, for his generosity in sharing his expertise; and Dr. Advait Jukar and Carlos Peredo, members of the Uhen Lab. I thank George Mason University and the Atmospheric, Oceanic, and Earth Sciences Department for providing me with a Graduate Teaching Assistant position. Lastly, I thank my family and friends: my parents, Rebecca and Rod, and my sister, Caroline; my best friend, EJ, and their parents Laura and Stan; my horses, Mikey, Pride, and Tess; and my pets, Willy and Ziggy. Without their love and support, I would not be where I am today.

TABLE OF CONTENTS

LIST OF TABLES

LIST OF FIGURES

LIST OF EQUATIONS

LIST OF ABBREVIATIONS

Smithsonian National Museum of Natural History ..... USNM
Paleobiology Database ..... PBDB

ABSTRACT

A NEW PLATANISTOID (CETACEA, ODONTOCETI) FROM THE NYE FORMATION OF OREGON

Margot D. Nelson, M.S.

George Mason University, 2019

Thesis Director: Mark D. Uhen

This thesis describes an early odontocete, here named *Perditicetus yaconensis*, gen. et. sp. nov., from the latest Oligocene-earliest Miocene Nye Formation in Oregon. I assign it to the Platanistoidea, a large superfamily of odontocetes whose sole surviving member is *Platanista gangetica*, the Ganges river dolphin. Despite the diversity of the Platanistoidea, it remains poorly understood and in need of revision. As one of the earliest-diverging clade of crown odontocetes, understanding their distribution, morphology, and phylogeny is crucial to understanding the radiation of basal crown odontocetes in the late Oligocene to the middle Miocene. *P. yaconensis*, represented by the holotype USNM 335224, possesses several synapomorphies of the Platanistoidea; however, similarity between *P. yaconensis* and other basal crown odontocetes suggests that these early odontocetes may be closer to the Platanistoidea than initially thought, especially those in the "*Chilcacetus* clade". The specimen's probable location in the

lower Nye Formation suggests that *P. yaconensis* is one of the older platanistoids known in the fossil record.

INTRODUCTION

The Odontoceti is the most diverse group of modern cetaceans, representing at least 60 known extant species (Mead and Brownell, 2005). Not only are odontocetes diverse, but they are also capable of incredible physiological feats: Cuvier's beaked whale, *Ziphius cavirostris*, is the deepest-diving marine mammal known (Schorr et al., 2014). Extant odontocetes demonstrate extraordinary intelligence and advanced social structures (Marino et al., 2007), including possible cultural learning, in the case of orcas learning how to strand themselves to capture pinnipeds (Guinet and Bouvier, 1995) and exhibiting cultural fads, such as tail-walking (Bossley et al., 2018). Their ability to echolocate has been a hallmark present in the earliest odontocetes (Geisler et al., 2014). The suite of unique characters present in odontocetes drives research into the evolution and systematics of this group, and to fully understand modern taxa, we must also study the fossil record. Fossil odontocetes are as fascinating as the species present today.

The narrative of the odontocete fossil record is as follows: the first odontocetes appear in the early Oligocene (Sanders and Geisler, 2015). Some of the earliest known odontocetes are *Simocetus* Fordyce, 2002, and *Ashleycetus* Sanders and Geisler, 2015, from the early Oligocene (Fordyce, 2002; Sanders and Geisler, 2015). Other stem odontocetes include the Xenorophidae, who are phylogenetically the first odontocetes to exhibit facial features indicative of echolocation (Geisler et al., 2014); and the

monospecific families Agorophiidae, Mirocetidae, and Patriocetidae. These stem odontocete families have a suite of plesiomorphic traits such as a heterodont dentition, limited polydonty (if present at all), and less telescoping of the facial bones (Marx et al., 2016). It is unclear if other families, such as the Squalodontidae and Waipatiidae, should be considered stem odontocetes, or part of crown Odontoceti; hypotheses of these families' place in the systematics of Odontoceti is discussed below.

By the late Oligocene, the earliest members of crown Odontoceti had appeared: the Physeteroidea (Mchedlidze, 1976), or sperm whales, and the Platanistoidea, which includes the extant Ganges river dolphin, *Platanista gangetica*. Unlike stem odontocetes such as the Xenorophidae and the Agorophiidae, these basal crown members displayed more derived traits such as polydonty, homodonty, and profound telescoping. From the late Oligocene to the early and middle Miocene, basal members of crown Odontoceti, such as the Platanistoidea and the Eurhinodelphinidae were dominant. Basal delphinidans such as the extinct Kentriodontidae and the river dolphin lineage Inioidea also appear during this time. Ziphiids first appear in the middle Miocene (Lambert and Louwye, 2006). However, by the late Miocene, the Delphinoidea (the oceanic dolphins) had appeared and diversified, and the basal crown odontocetes had largely disappeared (Marx et al., 2016). The reason for this decline of the basal lineages of odontocetes remains elusive, and a full understanding of the relationship between odontocetes is still lacking.

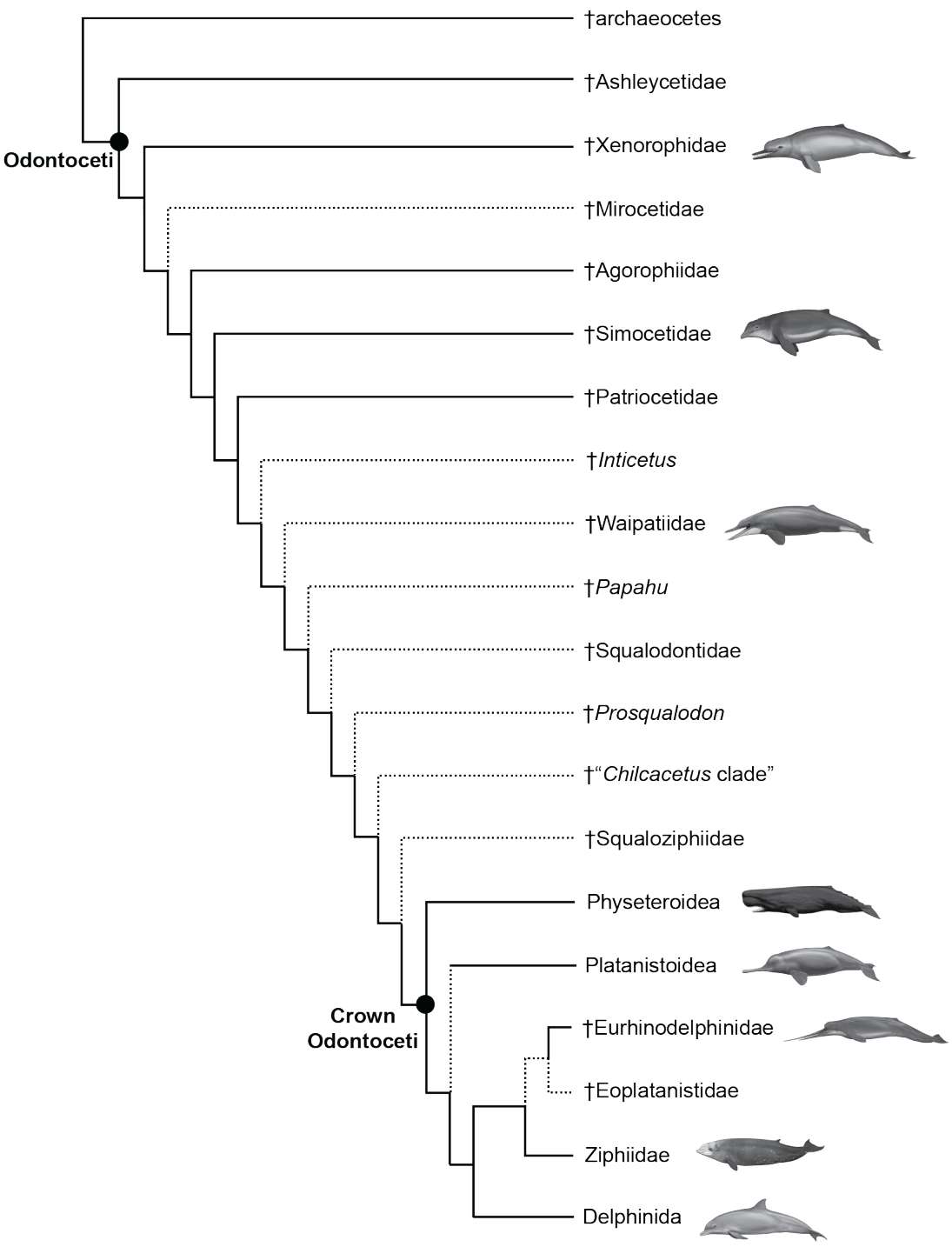

Figure 1 A simplified phylogeny of Odontoceti, modified from Marx et al. (2016). Stippled lines indicate taxa whose placement is uncertain (such as the Eoplatanistidae and Eurhinodelphinidae), or taxa that appear in crown Odontoceti in some phylogenies. Life reconstructions by C. Buell.

Systematics and Taxonomy of Basal Crown Odontocetes

Following is a description of the systematics and taxonomy of relevant families to this study. The following families have been placed in crown Odontoceti by various workers (see Figure 1). As these clades may form some of the earliest diverging branches of crown odontocetes, I will refer to these as basal crown odontocetes, differentiating them from demonstrably stem odontocetes such as *Simocetus* or the Xenorophiidae.

Lambert et al. (2015) first described *Chilcacetus cavirhinus*, and in their phylogenetic analysis derived an informal "*Chilcacetus* clade", containing *Chilcacetus*, *Macrodelphinus*, and the three species of *Argyrocetus*: *A. patagonicus* Lydekker 1894*, A. joaquinensis* Kellogg 1932*,* and *A. bakersfieldensis* Wilson 1935. The "*Chilcacetus* clade" appears to be supported by shared symplesiomorphies, thus Lambert et al. (2015) refrained from formally naming this group. One derived character, the dorsal surface of the nasal rising anterodorsally, was shared by all five taxa, but the authors noted that this character could be equivocal (Lambert et al., 2015). Subsequent phylogenies produced by Lambert et al. (2019) maintain support for the "*Chilcacetus* clade", as either just outside crown Odontoceti when a molecular backbone is used, or crownward of the Platanistoidea when using only morphological data.

Recently, a new family of potential basal crown odontocetes has been named, the Squaloziphiidae; this early Miocene family includes *Squaloziphius* de Muizon, 1991, and *Yaquinacetus* Lambert et al., 2019 (de Muizon, 1991; Lambert et al., 2019). The Squaloziphiidae are homodont polydont cetaceans found in the northeast Pacific. Their phylogenetic position is still unclear, but they appear to be either just outside crown

Odontoceti when a molecular backbone is used in phylogenetic analysis, or crownward of the Platanistoidea in analyses without a molecular backbone (Lambert et al., 2019). Synapomorphies of this family include an abrupt narrowing of the mesorostral canal, a laterally concave crest on the maxilla, and a massive postglenoid process of the squamosal. Other basal crown odontocetes include *Papahu* Aguirre-Fernández and Fordyce, 2014, a homodont polydont cetacean from the early Miocene of New Zealand, which could possibly be related to platanistoids, though phylogenetic analysis has placed it in stem Odontoceti (Aguirre-Fernández and Fordyce, 2014). There is also *Inticetus* Lambert et al., 2017, a heterodont odontocete from the early Miocene of Peru, which appears to be a stem odontocete allied with the Waipatiidae and Squalodontidae (Lambert et al., 2017); however, some analyses place *Inticetus* in crown Odontoceti if Waipatiidae and Squalodontidae also appear in the crown group.

The Platanistoidea is a superfamily that first appears in the fossil record in the late Oligocene and is considered one of the basalmost lineages. There is only one extant species in the superfamily, *Platanista gangetica* Lebeck 1801, or the Ganges River dolphin. During the Oligocene and Miocene, the Platanistoidea was far more diverse than it is today. Several odontocete families have been considered as members of the Platanistoidea; the Squalodontidae, Dalpiazinidae, Prosqualodontidae, Waipatiidae, Allodelphinidae, and Squalodelphinidae have all been considered platanistoids (Barnes, 2006; de Muizon, 1987; Fordyce, 1994).

The Squalodontidae are a family of odontocetes characterized by double-rooted cheek teeth with triangular, ornamented crowns. They are also characterized by an

elongate rostrum with large, procumbent incisors. The Squalodontidae were present from the late Oligocene to middle Miocene and have a wide distribution (Tanaka and Fordyce, 2014). The Squalodontidae is recognized as a "wastebasket taxon" containing many fragmentary odontocete fossils; only three genera, *Eosqualodon* Rothausen, 1968*,* *Squalodon* Grateloup, 1840*,* and *Phoberodon* Cabrera, 1926, are known from sufficiently diagnostic material (Dooley, 2005; Marx et al., 2016; Rothausen, 1968). The Dalpiazinidae, from the early Miocene of Italy, consists of one genus, *Dalpiazina* de Muizon, 1988, which is based on some fragmentary material (de Muizon, 1988, 1994). The Prosqualodontidae is another monogeneric family from the early Miocene of Australia and Argentina. *Prosqualodon* Lydekker 1894, is a short-snouted taxon with heterodont dentition (Cozzuol, 1996; Flynn, 1948).

The Waipatiidae were first described from the late Oligocene of New Zealand (Fordyce, 1994; Tanaka and Fordyce, 2014), but have been recorded in Australia, Malta, and Mexico (Bianucci et al., 2011; Fitzgerald, 2016; Gonzalez-Barba, 2007). They are characterized by a long, anteriorly attenuated rostrum with procumbent incisors and a series of small, double rooted cheek teeth. The family consists of *Waipatia* Fordyce 1994, and, putatively, *Otekaikea* Tanaka and Fordyce, 2014 (Tanaka and Fordyce, 2014; Tanaka and Fordyce, 2015a). In addition to *Waipatia* and *Otekaikea*, two other waipatiid-like genera have been described: *Awamokoa* Tanaka and Fordyce 2017, and *Urkudelphis* Tanaka et al., 2017 (Tanaka et al., 2017; Tanaka and Fordyce, 2017).

The Allodelphinidae are a small family from the Miocene of western North America and Japan (Barnes and Reynolds, 2009; Kimura and Barnes, 2016). They have

elongated rostra with many small, single-rooted teeth. The facial region lacks elevated crests. The family consists of five genera: *Allodelphis* Wilson, 1935*, Arktocara* Boersma and Pyenson, 2016, *Goedertius* Kimura and Barnes, 2016*, Ninjadelphis* Kimura and Barnes, 2016*,* and *Zarhinocetus* Barnes and Reynolds, 2009 (Boersma and Pyenson, 2016; Kimura and Barnes, 2016; Wilson, 1935). The Squalodelphinidae are small to medium-sized odontocetes from the early Miocene of Europe and both the Pacific and Atlantic coasts of the Americas (Bianucci et al., 2015). The squalodelphinids have a markedly V-shaped antorbital notch, a dorsoventrally expanded zygomatic process of the squamosal, a square-shaped pars cochlearis of the periotic, and an elongate median furrow of the tympanic bulla. Squalodelphinids also have a thickened maxilla over the orbit, and single-rooted teeth. There are currently six genera: *Huaridelphis* Lambert et al., 2014*, Medocinia* de Muizon, 1988*, Notocetus* Moreno, 1892*, Phocageneus* Leidy, 1869, *Macrosqualodelphis* Bianucci et al., 2018*,* and *Squalodelphis* Dal Piaz, 1917 (Bianucci et al., 2018; de Muizon, 1987; Lambert et al., 2014).

The Platanistidae, the sole extant family in Platanistoidea, has a fossil record from the early to late Miocene. There are no unequivocal fossils from the Pliocene. Platanistids have been found in marine rocks from Europe, Korea, and North America (Barnes, 2006; Lee et al., 2012); freshwater or estuarine occurrences have been reported from Peruvian Amazonia and the southeast United States (Bianucci et al., 2013; Hulbert and Whitmore, 2006). Platanistids had elongate rostra with many single-rooted teeth, a deep lateral groove on the lateral side of the rostrum and mandible, conspicuous facial crests, a dorsoventrally expanded zygomatic process (as seen in squalodelphinids), and a hook-

like articular process on the periotic (de Muizon, 1987). Genera included in the Platanistidae include *Platanista, Pomatodelphis* Allen, 1921*, Zarhachis* Cope, 1868*, Dilophodelphis* Boersma et al., 2017*,* and *Araeodelphis* Kellogg, 1957 (Barnes, 2006; Boersma et al., 2017; Godfrey et al., 2017; Kellogg, 1957).

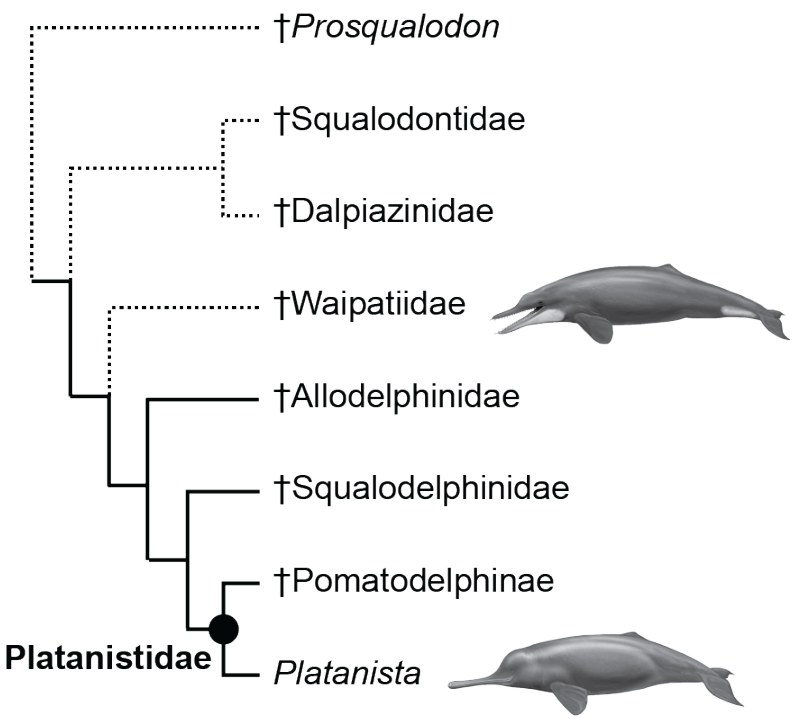

Figure 2 A simplified phylogeny of the Platanistoidea, modified from Marx (2016). Dashed lines indicate taxa that appear as stem odontocetes in some phylogenetic analyses. Life reconstructions by C. Buell.

Other basal crown odontocetes include the Eurhinodelphinidae and the Eoplatanistidae. These families have no extant species. The Eoplatanistidae is a monogeneric family from the early Miocene of Italy. *Eoplatanista* Dal Piaz, 1916, is a small odontocete with a long rostrum and numerous single-rooted teeth. It is

characterized by mesial and distal keels on the teeth, the presence of a longitudinal groove on the rostrum and mandible (superficially similar to that of allodelphinids and platanistoids), a flat skull vertex with exposed frontals, and no median furrow on the tympanic bulla (de Muizon, 1988). *Eoplatanista* is possibly the sister group of eurhinodelphinids, but other recent phylogenies placed the genus outside a clade containing Eurhinodelphinidae, Platanistoidea, Ziphiidae, and Delphinoidea (de Muizon, 1991; Lambert et al., 2015).

The Eurhinodelphinidae is a highly distinctive family with very elongated rostra. They are known from the early to middle Miocene of Europe and the east coast of North America (Lambert, 2005a). Eurhinodelphinids are distinguished by an endentulous portion of the premaxilla that can be half the length of the rostrum, and a mandible that is much shorter than the upper jaw. The rostrum and mandible have lateral grooves, similar to that of *Eoplatanista* (Lambert, 2005a). The function of the elongated, edentulous premaxilla remains unknown, though a recent study suggests that hyper-longirostry may be an adaptation for prey capture (McCurry and Pyenson, 2018). Who belongs in the Eurhinodelphinidae is unclear; the Paleobiology Database lists *Eurhinodelphis* Van Beneden and Gervais, 1880, *Schizodelphis* Gervais, 1861, *Xiphiacetus* Lambert, 2005b, *Ziphiodelphis* Dal Piaz, 1908, *Mycteriacetus* Lambert, 2004, *Ceterhinops* Leidy, 1877 , *Iniopsis* Lydekker, 1892 , *Phocaenopsis* Huxley, 1859 , and *Vanbreenia* Bianucci and Landini, 2002 as members of the family. However, the only unequivocal synapomorphies of Eurhinodelphinidae are rostral; so taxa that do not preserve the rostrum can only tentatively be assigned to this family (Lambert, pers. comm.). Only

Eurhinodelphis, Schizodelphis, Xiphiacetus, Ziphiodelphis, and *Mycteriacetus* have associated rostra (Lambert, 2004, 2005a, b; Marx et al., 2016). Former members of the family include *Argyrocetus* and *Macrodelphinus*, who are now considered members of the "*Chilcacetus* clade" (Lambert et al., 2015). There is little consensus regarding the phylogenetic placement of Eurhinodelphinidae. Sister-group relationships with Eoplatanistidae, Platanistoidea, Delphinoidea, or Ziphiidae, or a lineage basal to these clades, have been suggested (de Muizon, 1991; Lambert, 2005a; Lambert et al., 2015).

The Eoplatanistidae is a monogeneric family from the early Miocene of Italy. *Eoplatanista* Dal Piaz, 1916, is a small odontocete with a long rostrum and numerous single-rooted teeth. It is characterized by mesial and distal keels on the teeth, the presence of a longitudinal groove on the rostrum and mandible (superficially similar to that of allodelphinids and platanistoids), a flat skull vertex with exposed frontals, and no median furrow on the tympanic bulla (de Muizon, 1988). *Eoplatanista* is possibly the sister group of eurhinodelphinids, but other recent phylogenies placed the genus outside a clade containing Eurhinodelphinidae, Platanistoidea, Ziphiidae, and Delphinoidea (de Muizon, 1991; Lambert et al., 2015).

If there is anything to be gained from discussion of putative basal crown odontocetes, it is that there is an incredible diversity and disparity, but that phylogenetic relationships are still tenuous, and it is unclear which taxa belong in crown Odontoceti.

Systematics of the Platanistoidea

The modern river dolphins were originally considered a monophyletic group containing the Ganges river dolphin, *Platanista gangetica*, the Amazonian river dolphin,

Inia geoffrensis Blainville, 1817, the recently extinct Yangtze river dolphin, *Lipotes vexillifer* Miller, 1918, and the Fransiscana, *Pontoporia blainvillei* Gervais and d'Orbigny, 1844, as well as fossil taxa such as *Zarhachis*, *Ischyorhynchus* Ameghino, 1891, and *Pontistes* Burmeister, 1885 (Simpson, 1945). However, studies of morphological and molecular data support the paraphyly of this definition, and *Platanista* is not closely related to *Lipotes, Pontoporia,* and *Inia* (Cassens et al., 2000; Geisler et al., 2011; Hamilton et al., 2001). Furthermore, molecular divergence times support different origination times for the Platanistidae, the Inioidea, and the Lipotidae (McGowen et al., 2009). Better understanding of evolutionary relationships between the river dolphins has led to the redefinition discussed in the previous section, that the Platanistoidea contains all odontocetes more closely related to *Platanista* than any other odontocete. The latter taxa are allied with oceanic dolphins, although some strictly morphological studies argue the opposite, and state that the various river dolphin taxa are closely related (Barnes, 2006; Pyenson et al., 2015). It is more likely that the morphological similarities between the four river dolphin taxa are due to convergent evolution.

P. gangetica is highly derived and exhibits unique to a riverine habitat such as a flexible neck, wide, paddle-like flippers, and extremely reduced eyes (Cassens et al., 2000). However, the transition from a marine to riverine transition in the Platanistoidea is shrouded in mystery. While a few fossils of platanistoids have been found in fluvial or estuarine deposits (Barnes, 2006; Hulbert and Whitmore, 2006), the majority of fossil platanistoids were living in marine environments.

Several definitions have been considered for the Platanistoidea. De Muizon (1987) considered Platanistoidea to be the Squalodontidae, the Squalodelphinidae, and the Platanistidae; he united these three taxa with two synapomorphies: 1) the reduction of the coracoid process of the scapula, and 2) the lack of the supraspinous fossa of the scapula. This initial diagnosis was modified to include a deep subcircular fossa located dorsal to the spiny process of the squamosal, an articular process or rim on the periotic, and the migration of the palatines dorsolaterally (de Muizon, 1994). Fordyce (1994) added two new synapomorphies in his description of *Waipatia maerewhenua*, the anterior process of the periotic roughly cylindrical in cross section, and the anterior process smoothly deflected ventrally. This diagnosis eliminated synapomorphies based on the palatines and noted that scapular characters were equivocal. This result placed the Waipatiidae within the Platanistoidea in addition to the Squalodontidae, Squalodelphinidae, and Platanistidae.

The Lambert et al. (2014) description of *Huaridelphis* listed these synapomorphies for the Platanistoidea, based on character states in their phylogenetic analysis: deeply grooved rostral suture between premaxilla and maxilla, elevation of the antorbital region higher than the rostral base, widening of cranium, presence of a deep fossa in orbit roof, vertex shifted to the left compared to the sagittal plane of the skull, reduction of ventral exposure of palatine, hamular fossa of the pterygoid sinus extended anteriorly on the palatal surface of rostrum, presence of articular rim on the periotic, elongation of anterior spine on the tympanic bulla, loss of double rooted teeth, and tooth count greater than 25. Lambert et al.'s (2014) analysis did not recover de Muizon's

(1987) scapular synapomorphies. This resulted in a Platanistoidea that did not contain the Squalodontidae and instead included the Allodelphinidae, Squalodelphinidae, and Platanistidae. Other work using larger matrices placed the Squalodontidae with other stem odontocetes (Geisler et al., 2011).

Tanaka and Fordyce (2015b), in contrast, based Platanistoidea on six synapomorphies recovered in their phylogenetic analyses: presence of posterior dorsal infraorbital foramina of maxilla, C-shaped or weakly curved parabullary sulcus, presence of articular rim on the periotic, presence of anterior spine of the tympanic bulla, presence of anterolateral convexity of the tympanic bulla, and presence of the ventral groove of the tympanic bulla anteriorly. These synapomorphies united the Waipatiidae, Squalodelphinidae, and Platanistidae as the Platanistoidea. In their phylogenetic analysis, Boersma et al. (2017) recovered six synapomorphies: emargination of the posterior edge of zygomatic process by neck muscle fossae, presence of suprameatal pit of squamosal, presence of posterior periotic fossa of squamosal, lateral groove affecting dorsal view of periotic, anteroposterior ridge on dorsal side of periotic, and ventral surface of posterior process of periotic concave or convex perpendicular to its long axis. This resulted in a Platanistoidea that contains the Allodelphinidae, Squalodelphinidae, and Platanistidae. This Platanistoidea, Allodelphinidae + Squalodelphinidae + Platanistidae, is emerging as the consensus view (see Figure 2), especially since Waipatiidae and Squalodontidae appear as stem odontocetes in many phylogenies. There is consensus amongst fossil-based phylogenies that the Squalodelphinidae is the sister family of the Platanistidae.

Here, I present a new genus and species of the Platantistoidea from the late Oligocene-early Miocene Nye Formation of Oregon, named *Perditicetus yaconensis*. This genus and species is represented by the holotype specimen USNM 335224, housed at the Smithsonian National Museum of Natural History (NMNH). The holotype is a nearly complete skull with associated left periotic and right tympanic. Synapomorphies present indicate that this new basal crown odontocete belongs in the Platanistoidea, likely as the basalmost taxon in this enigmatic superfamily. I obtained this result consistently in all phylogenetic analyses. Though *Perditicetus* is a platanistoid, it bears similarities to other basal crown odontocetes in the "*Chilcacetus* clade", *Chilcacetus* and *Argyrocetus*, suggesting that these taxa may be more closely related to platanistoids than initially thought.

MATERIALS AND METHODS

Description and Comparison

Mead and Fordyce (2009) is considered the standard for anatomical terminology of the odontocete skull. The anatomical description of USNM 335224 will follow the terminology laid out in this publication. USNM 335224 was compared to several other odontocetes, such as the putative platanistoids *Waipatia* and *Squalodon calvertensis,* eurhinodelphinids such as *Argyrocetus, Eurhinodelphis, Schizodelphis,* and *Xiphiacetus,* and platanistoids *Allodelphis, Araeodelphis, Pomatodelphis,* and *Zarhachis*.

Specimens Observed

Notocetus sp. (USNM 639719, USNM 207286); *Phocageneus* sp. (USNM 317651); *Phocageneus venustus* (USNM 21039); *Pomatodelphis bobengi* (USNM 360052); *Squalodon calvertensis* (USNM 10949, 529426); cast of *Waipatia maerewhenua* (USNM 508061); *Zarhachis flagellator* (USNM 299945); *Zarhachis* sp. (USNM 214759).

Phylogenetic Methods

USNM 335224 was included in several phylogenetic analyses to elucidate its phylogenetic position within Odontoceti. All three analyses were run in PAUP*, or Phylogenetic Analysis Using Parsimony (Swofford, 2002). All heuristic searches were conducted using ACCTRAN optimization and the Tree Bisection and Reconnection

(TBR) algorithm. After heuristic searches were conducted, both a strict consensus, where only nodes present in all most parsimonious trees are displayed, and a 50% majority-rule consensus, where nodes present in 50% or more of most parsimonious trees, were computed. Using consensus trees enables the viewer to see a condensed version of most parsimonious trees, especially in analyses where the number of most parsimonious trees is quite large. Strict consensus is the most conservative approach, but a majority-rule consensus usually produces a more resolved tree. It has become standard to depict both strict and majority-rule consensus trees.

The first used was the matrix published with *Arktocara yakataga* by Boersma and Pyenson (2016), modified from the matrix used in Tanaka and Fordyce (Tanaka and Fordyce, 2015a). This matrix is one of the largest and most comprehensive matrices of Odontoceti, and contains a wide variety of stem odontocetes, as well as representatives from all major members of crown Odontoceti. I will refer to the *Arktocara* phylogenetic analysis as Analysis 1. This matrix has 87 taxa, including USNM 335224, and 292 characters, all unordered and equally weighted. Due to the large size of this matrix, I performed a heuristic search using simple stepwise addition, with *Georgiacetus vogtlensis* Hulbert et al., 1998, as outgroup.

The second analysis performed, referred to as Analysis 2, used the matrix published with *Dilophodelphis fordycei* by Boersma et al. (2017); this matrix was originally published with the description of *Huaridelphis* by Lambert et al. (2014) and modified by Godfrey et al. (2017) in their publication of *Araeodelphis*. This was a much smaller analysis, with 21 taxa and 67 characters, all considered unordered and unweighted. This

phylogenetic analysis focuses strongly on relationships within the Platanistoidea and contains almost all known members of the Allodelphinidae, Squalodelphinidae, and Platanistidae. However, it is important to note that this analysis lacks more crownward taxa such as the Delphinida. *Zygorhiza kochii* True, 1908, was used as the outgroup. I ran this heuristic search both using simple stepwise addition, and random stepwise addition with 10,000 replicates. Both heuristic searches had the same results.

The last analysis, henceforth referred to as Analysis 3, was the matrix published with *Chilcacetus cavirhinus* by Lambert et al. (2015). This matrix has 36 taxa and 77 characters; all characters were unordered. *Zygorhiza* was used as the outgroup. This analysis contains a diversity of basal crown odontocetes not found in other phylogenetic analyses, such as *Argyrocetus* and *Macrodelphinus*, as well as many platanistoids and representatives of more crownward clades. I initially performed this analysis using a heuristic search with simple stepwise addition, which resulted in a poorly resolved tree. To replicate the more resolved tree in the original publication, I followed the methods exactly as described by Lambert et al. (2015): I ran a heuristic search with simple stepwise addition, and down-weighted homoplastic characters following the method of (Goloboff, 1993), using the default value k=3. The Goloboff method is an implied weighting method that resolves character conflict in favor of characters that are more likely to be homologous.

Body Size Estimation

To estimate the body size of USNM 335224, I used the method outlined by Pyenson and Sponberg (2011). As this specimen is missing the apex of the rostrum, the occipital

condyles, and part of the right exoccipital, I could not use the partial least squares (PLS) equation, which requires measurements of the condylobasal length, occipital condyle breadth, and exoccipital width. Instead, I used the equation for bizygomatic width (BIZYG) for stem Platanistoidea (Equation 1). This measurement is taken from the widest lateral margin of the left zygomatic process to the right.

Photography and Figures

Digital photography was done at the Smithsonian National Museum of Natural History, where USNM 335224 is housed. The specimen was coated with ammonium chloride, a solid that was sublimated onto the specimen to whiten it. The tympanic was photographed in dorsal, medial, posterior and ventral view, the periotic was photographed in ventral, lateral, dorsal, and medial view, and the skull was photographed in dorsal, posterior, ventral, and lateral view. The photos were masked using Adobe Photoshop and line drawings of USNM 335224 were drawn in Adobe Illustrator. Data for Platanistoidea was downloaded from the Paleobiology Database (PBDB), and data for the geology of Oregon was downloaded from the Oregon Department of Geology and Mineral Industries. Tectonic reconstructions were made in Gplates; all map figures were constructed in ArcGIS.

Equation 1 Body size estimation using bizygomatic width, for stem Platanistoidea. From Pyenson and Sponberg (2011).

$$\log(L) = 0.92 * (\log(\text{BIZYG}) - 1.51) + 2.49$$

SYSTEMATIC PALEONTOLOGY

Order CETACEA Brisson 1792

PELAGICETI Uhen 2008

NEOCETI Fordyce and de Muizon 2001

ODONTOCETI Flower 1867

PLATANISTOIDEA Gray 1863

Family incertae sedis

PERDITICETUS gen. nov.

Type species— *Perditicetus yaconensis*, sp. nov.

Diagnosis— as for the type and only species.

Etymology— From the Latin word, "*perditus*", meaning lost, a reference to the type locality south of Lost Creek; "*cetus*", being the Latin word for whale.

PERDITICETUS YACONENSIS sp. nov.

Holotype— USNM 335224, a nearly complete skull lacking the tip of the rostrum and occipital condyles, a complete left periotic, and incomplete right tympanic bulla.

Diagnosis— *Perditicetus yaconensis* is a small odontocete with a long rostrum comprising >55% of the skull length. Skull is slightly asymmetrical; alveoli preserved on the maxilla indicate a homodont polydont dentition. It is placed in the Platanistoidea based on the following synapomorphies: emargination of the posterior edge of the

zygomatic process of the squamosal, a deep subcircular fossa in the squamosal, widening of the cranium where the cranium is distinctly shorter than wide, the division of the periotic fossa into anterior and posterior fossae, an articular rim of the periotic, lateral groove affecting the dorsal profile of the periotic so that it appears sigmoidal in dorsal view, and a weakly curved parabullary sulcus. *Perditicetus yaconensis* differs from the Allodelphinidae, Squalodelphinidae, and Platanistidae in the vertex being roughly in the sagittal plane, possessing a reduced lateral lamina that does not contact the falciform process of the squamosal, in the premaxillary foramen situated posterior to the antorbital notch, and in the separation of the zygomatic process of the squamosal from the postorbital process of the frontal, and in the anterior projection of the nasal giving the external nares a heart-shaped appearance. It further differs from the Allodelphinidae in lacking a deep lateral groove along the rostrum, in the constriction of the mesorostral canal being at the level of the premaxillary sac fossa, in the blunt, rounded postglenoid process, and in the dorsal edge of the temporal fossa being level with the vertex. *P. yaconensis* differs from the Squalodelphinidae and Platanistidae in lacking an supraorbital thickening or crest, in lacking V-shaped left antorbital notch, in the dorsal surface of the antorbital process being level with the rostrum base, in the nasal partly overhanging the external nares, in the posterior dorsal infraorbital foramen located lateral to the premaxillary sac fossa, in the absence of an orbital fossa for the pterygoid sinus, in the reduced lateral lamina, and lacking a square-shaped profile to the pars cochlearis in ventral view. It further differs from the Platanistidae in lacking a lateral groove between the premaxilla and the maxilla.

Etymology— After the Yacona people, original inhabitants of the type locality along the Oregon coast in Lincoln County.

Type Locality— USNM 335224 was collected by Douglas Emlong in March of 1971; it was recorded as Emlong 744 in his notes. D. Emlong's field data states that the specimen was found *in situ* 0.5 miles south of the mouth of Lost Creek, in front of Wandamere Resort (Fig. 1). This resort no longer exists. Lost Creek is located south of Newport, in Lincoln County, Oregon. Georeferenced coordinates for the type locality are 44.535717° N, 124.075019° W. Paleobiology Database collection: Wandamere Resort, 200294.

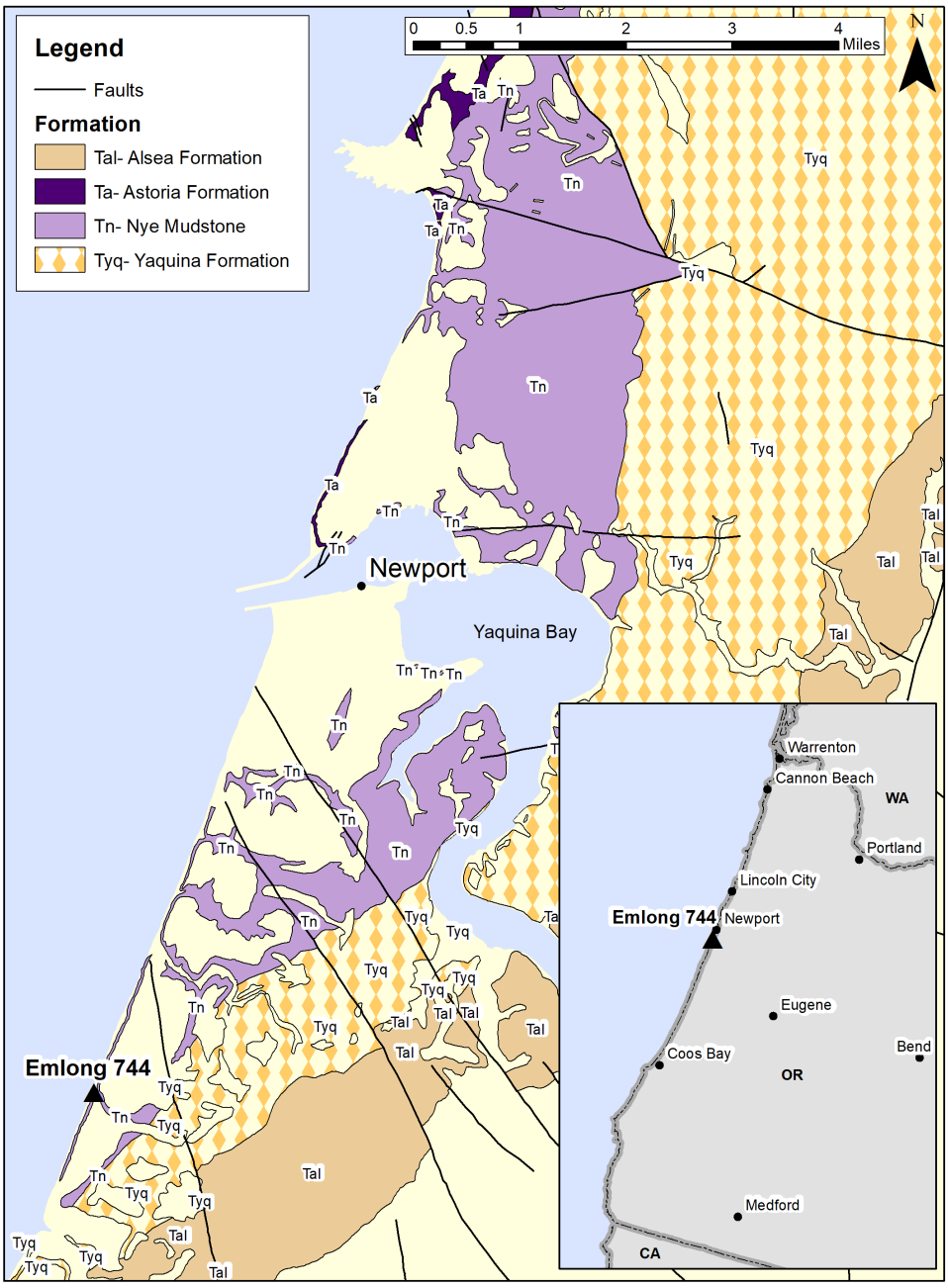

Figure 3 The location of the type locality of *Perditicetus yaconensis* (Emlong 744) and the surrounding geology. Note the proximity of the type locality to the contact with the underlying Yaquina Formation.

Age and Stratigraphy— The type locality is situated in the Nye Formation, also known informally as the Nye Mudstone. The Nye Formation was first referred to in the literature as the Nye Shale by Smith (1926); Schenck (1927) designated a type locality in Newport, Oregon at Nye Beach from which the Nye Formation gets its name.

The Nye Formation is composed of medium to dark olive-grey, massive mudstone and siltstone; it is organic-rich and freshly broken samples smell like petroleum (Prothero et al., 2001). Calcitic and dolomitic concretions are present. The Nye conformably overlies the late Oligocene Yaquina Formation, and is unconformably overlain by the Astoria Formation, which is early to middle Miocene in age (Fig. 2). The benthic foraminifera present in the Nye Formation suggest a depositional environment of bathyal depths (300-600 m) (Snavely et al., 1964); planktonic foraminifera are sparse, but species present indicate cold waters analogous to the cool-water masses seen off the Oregon coast today (McKeel and Lipps, 1972). Benthic foraminifera stratigraphy place the Nye Formation within the Zemorrian to Saucesian stages, which correspond to the Chattian to Aquitanian stages (Nesbitt, 2018). Molluscan stratigraphy places the Nye Formation in the Pillarian stage, which is thought to correspond with the Aquitanian (Addicott, 1976). Magnetostratigraphic studies support the ages obtained from foraminiferal and molluscan stratigraphy; Prothero et al. (2001) place the age of the Nye Formation at 28-23 Ma.

The geologic map drawn by drawn by Vokes et al. (1949) depicts the southernmost extent of the Astoria Formation as approximately one mile south of the mouth of Yaquina Bay; in cross-section, the Yaquina, Nye, and Astoria Formations dip gently to the west. My interpretation of this data is that the Nye Formation is younger as

one moves west; this assessment is confirmed by younger magnetostratigraphic ages in the west as opposed to east (Prothero et al, 2001). Given that the outcrops near Lost Creek are closer to the contact with the underlying Yaquina Formation than to the contact with the overlying Astoria Formation, the type locality of *Perditicetus* is likely closer to the bottom of the formation. I contend that USNM 335224 is from the Chattian based on this interpretation; however, a foraminiferal study of type locality would be required to determine if the locality has a Zemorrian (Chattian) or a Saucesian (Aquitanian) assemblage.

Other marine mammals present in the Nye Formation include *Desmostylus hesperus* Marsh, 1888 (Domning, 2008), a halitheriine sirenian (Domning and Ray, 1986), pinnipeds such as *Enaliarctos* Mitchell and Tedford, 1973, and *Pinnarctidion* Barnes, 1979 (Berta, 1991, 1994), the "beach bear" *Kolponomos* Stirton, 1960 (Tedford et al., 1994), the squaloziphiid *Yaquinacetus* (Lambert et al., 2019), and the platanistoid *Goedertius oregonensis* (Kimura and Barnes, 2016).

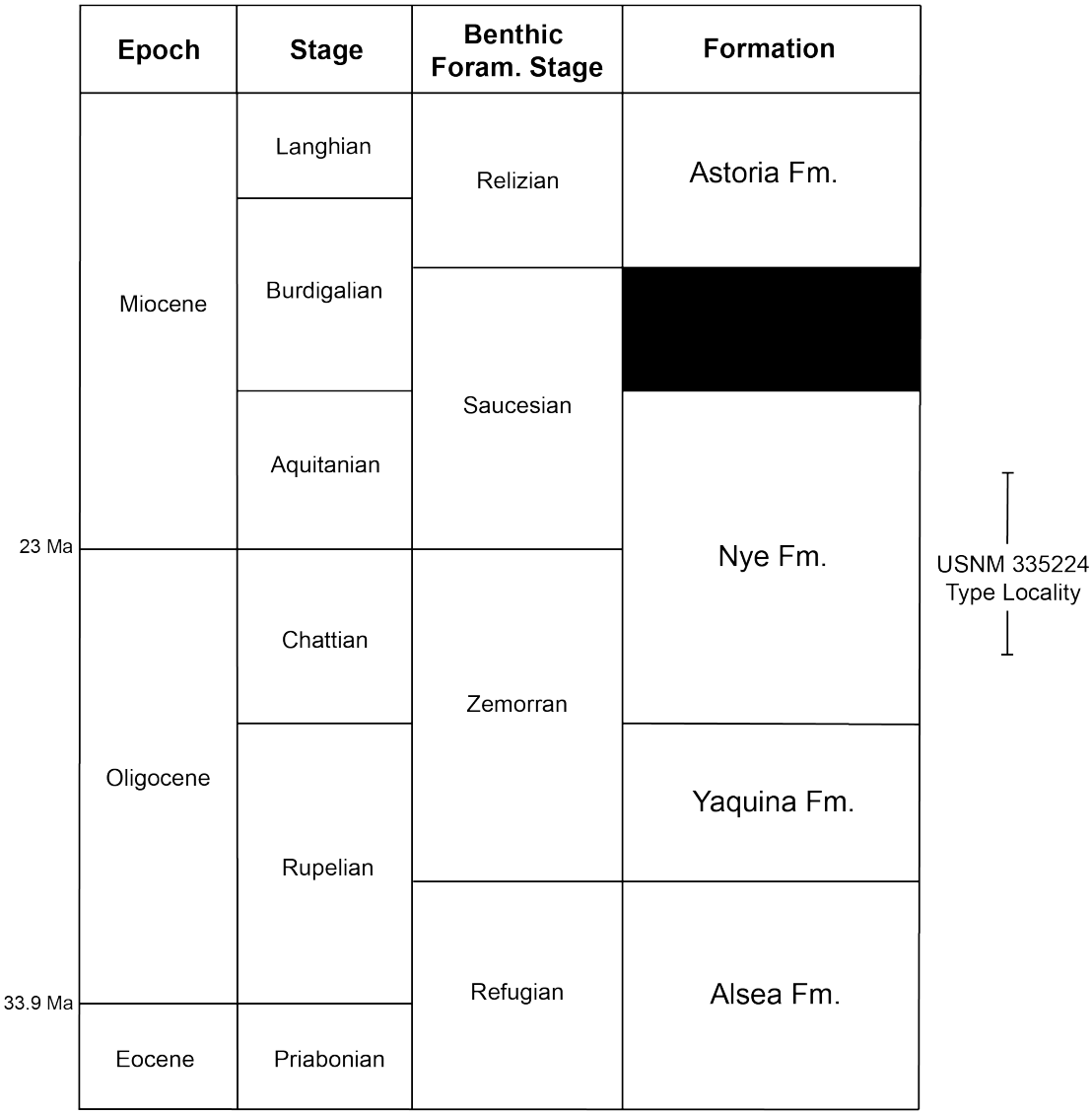

Figure 4 A stratigraphic column of the units in the Newport, OR area. Dates for the Eocene-Oligocene and Oligocene-Miocene boundaries are from Gradstein et al. (2004). The blacked-out area represents the unconformity between the Nye Formation and the Astoria Formation.

DESCRIPTION

General Description

The skull of the holotype USNM 335224 is nearly complete; it lacks occipital condyles, the apex of the rostrum, the jugals, and the ventral surface of the lacrimals. There is major damage to both parietals, and the right exoccipital and squamosal. There appears to be no diagenetic distortion. The skull is slightly asymmetrical. The skull is small, with a condylobasal length of at least 378 mm; this measurement is a minimum estimate since the apex of the rostrum could extend much further. Body size estimate for the holotype is 2.06 m (bizygomatic width 20.8 cm). The majority of sutures in USNM 335224 are fused, and maxillary alveoli are ossified; these features indicate that USNM 335224 was an adult. The left periotic and right tympanic bulla were prepared out of the skull.

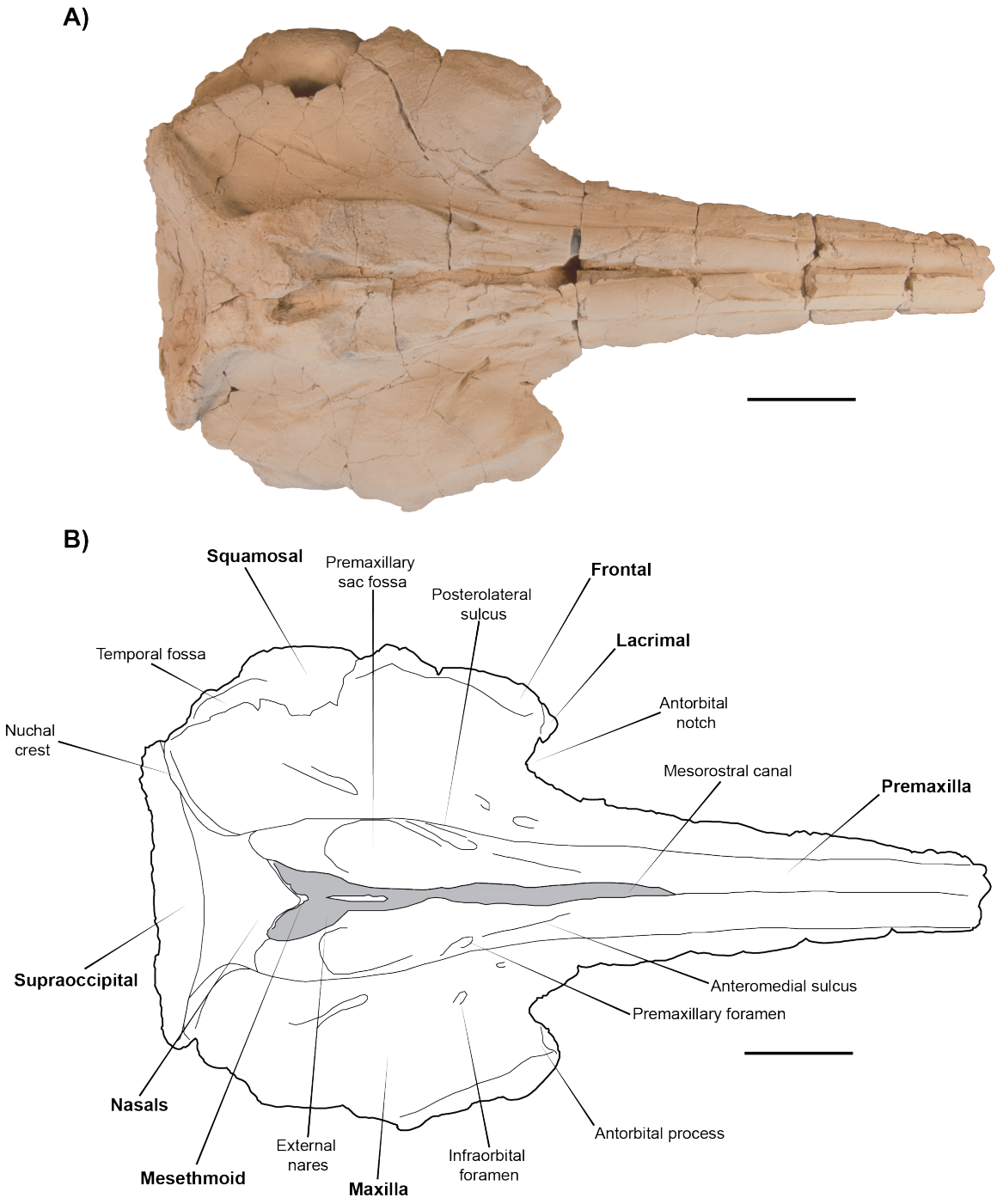

Figure 5 Photo (a) and line drawing (b) of the skull of *Perditicetus yaconensis*, USNM 335224 (holotype), dorsal view. The names of bones are in bold type; grey areas indicate either broken surfaces or infilling matrix. Scale bar = 5 cm. Note the slight asymmetry, the temporal fossa roofed over by the maxilla and frontal, and the cranium wider than it is long.

Cranium

The cranium, defined as the skull posterior to the antorbital notches, is square-shaped, being about as long as it is wide. In lateral view, the supraorbital process is only slightly elevated above the base of the rostrum. The narial passages are subvertical and the external nares open at the level of the postorbital process of the frontal. The facial region is slightly concave; the vertex is elevated approximately 60 mm above the base of the rostrum. In dorsal view, the maxillae and frontals roof over the anterior portion of the temporal fossa but leaves the supramastoid crest and the posterior portion of the temporal fossa exposed. The facial region as a result appears somewhat trapezoidal, similar to the condition observed in other early odontocetes such as *Waipatia* and *Chilcacetus*; the extent of the lateral margin of the ascending process of the maxilla resembles that of the squalodelphinids *Huaridelphis* and *Notocetus*. There is a thin but well-developed temporal crest; the zygomatic process of the squamosal and the postorbital process of the frontal are close together, separated by only 5 mm. There is a reduced intertemporal constriction, with very little, if any, of the parietals exposed in dorsal view. The vertex of the skull is square-shaped and flat. The basicranium has suffered some significant damage: there are 2 large holes on the left and one large hole on the right, exposing the endocranial space.

Rostrum

The rostrum is long, comprising approximately 50% of the condylobasal length and likely extended further. In dorsal view, the premaxillae contact each other for roughly half the rostrum's length. The mesorostral canal is narrow, reaching a maximum

of 10 mm in width, and is constricted anterior to the external nares. This contrasts the open condition of the mesorostral canal seen in more basal odontocetes *Squalodon* and *Waipatia*. There is a prominent antorbital notch, which transmits the facial nerve. There is only slight asymmetry in the shape of the antorbital notches. This is different from what is seen in squalodelphinids, which possess a left antorbital notch that is narrower ("V" shaped) in dorsal view than the right antorbital notch. The antorbital notch also differs from the condition seen in *Argyrocetus joaquinensis* in that the right antorbital notch is markedly shallower than the left. The antorbital processes, formed by the lacrimal, maxilla, and the anterior-most frontal, extend to form the lateral margin of the antorbital notch. Anterior to the antorbital notch, the lateral margin of the maxilla flares out to form the maxillary flange. In lateral view, the premaxilla forms the dorsal profile. In ventral view, the surface of the rostrum is mainly formed by the maxilla, with the vomer visible in the anterior portion. The lateral margin of the ventral surface is poorly preserved. The anterior portion of the ventral surface is grooved, whereas the posterior portion is convex. There is a slight palatal ridge where the palatine contacts the maxilla.

Premaxilla

In dorsal view, the premaxillae maintain a uniform thickness along the rostrum to the level of the antorbital notch, at which point they expand to accommodate the premaxillary sac fossa. On the posterior third of the rostrum, the suture between the premaxilla and the maxilla appears tight, possibly fused; however, on the anterior portion of the rostrum, there is infilling of matrix in the suture between the maxilla and premaxilla, indicating that this suture may have been unfused (Fig. 3). There is no lateral

groove marking the suture between the premaxilla and maxilla, differing from allodelphinids, platanistids, eurhinodelphinids, and eoplatanistids. The dorsal profile of the premaxillae is flat along the rostrum. The premaxillae contact each other for half the anterior length of the rostrum and the mesorostral groove is exposed on the posterior half. This contact between the premaxillae may not have been sutural based on the overlapping of the right premaxilla over the left. The mesorostral groove is widest at the level of the antorbital notch and abruptly narrows at the level of the anterior edge of the premaxillary sac fossa. There is one premaxillary foramen on the left and right premaxilla located posterior to the antorbital notch; the left premaxillary foramen is situated posterior to the right premaxillary foramen. The placement of the premaxillary foramen is similar to the position seen in *Squaloziphius*. In *Waipatia*, *Xiphiacetus*, and most other platanistoids *sensu* Lambert et al., (2014) the premaxillary foramen is situated anterior to the antorbital notch; in *Chilcacetus* and *Argyrocetus joaquinensis*, the premaxillary foramen is situated at the level of the anterior notch. The premaxillary foramina are subequal in size, and transmit the maxillary nerve, a branch of the trigeminal nerve. The anteromedial sulcus is visible but poorly defined; this sulcus forms the prenarial triangle, the origin for the nasal plug muscle. The posterolateral sulcus creates a thin lateral edge of the ascending process of the premaxilla, which overhangs the maxilla. There is no apparent posteromedial sulcus present. The premaxillary sac fossa is smooth and transversely flat. The premaxillae are widest at the prenarial constriction just anterior to the external nares, at which point the premaxillae constrict until they contact the anterolateral edge of the nasals. The suture between the premaxilla and nasal is indistinct. Unlike *Waipatia,*

Otekaikea, and *Papahu*, there is no bifurcation of the premaxilla at the apex. The lateral margin of the premaxilla is thickened and is elevated above the ascending process of the maxilla. The premaxillae are not exposed in ventral view.

Maxilla

On the dorsal surface of the maxilla, there is noted asymmetry in the location of the infraorbital foramina (responsible for transmitting the maxillary nerve) on the left and right maxillae. On the right maxilla, a foramen is present on the dorsal surface of the maxillary flange anterior to the antorbital notch. There is a second foramen located posteromedial to the antorbital notch. On the left maxilla, there is a foramen at the level of the antorbital notch with a sulcus that extends anteriorly along the maxillary flange. The second is located slightly posteromedial to the antorbital notch. There is one dorsal infraorbital foramen on each ascending process of the maxilla, accompanied by sulci that extend both anteromedially and posterolaterally. At the vertex, the maxilla appears to contact the supraoccipital and forms part of the nuchal crest. There appears to be asymmetry in the contact between the maxilla and the frontal; on the left side the suture between maxilla and frontal on the dorsal surface is indistinct, whereas on the right side the suture is thickened and appears almost crenulated. On the right side, the maxilla appears to overlap the lacrimal, but does not completely cover it. The maxilla is not thickened over the orbit in lateral view. In ventral view, the maxilla forms most of the surface of the rostrum. The maxilla extends back to the level of the internal opening of the infraorbital foramen. There are 14 well preserved alveoli on the maxilla, all subequal in size. This demonstrates that *Perditicetus* had single-rooted teeth. The alveoli appear to

terminate well anterior to the maxillary flange and the antorbital notch, however this may be due to the poor preservation of the lateral margin of the maxilla. The maxilla contacts the palatine along a weakly-defined palatal sulcus. Between the lateral margin of the palatine and the ventral infraorbital foramen, there appears to be an oblique crest, similar to that described by Lambert et al. (2015) in *Chilcacetus*. This feature appears in other odontocetes and may indicate the origin of the internal or external pterygoid muscles. The maxilla appears to form the wall of the antorbital notch, though the lacrimal may also contribute.

Palatine

The palatine is long and V-shaped in ventral view. They are widest posteriorly and taper to a point approximately 30 mm anterior to the antorbital notch, though they may extend further (Fig. 4). The palatine and maxilla appear to be fused. If a palatal foramen is present, it has been obscured by slight damage to the ventral surface. The left and right palatines are separated medially by the maxillae for approximately 30 mm backwards from the anterior point of the palatine, similar to the morphology seen in *Chilcacetus*. Together, the medial contacts between the left and right maxillae and between the left and right palatines form a keel-like ridge that extends 50 mm anterior to the antorbital notch. This morphology differs from that seen in *Squalodon* and *Waipatia* and could be related to an elongated rostrum (Lambert et al., 2015). The palatine does not appear to be exposed in the pterygoid sinus fossa. The suture between the palatine and pterygoid is indistinct, likely fused. There is no lateral lamina present.

Pterygoid

The anterior portion of the pterygoid is well preserved; however, the hamular process of the pterygoid is missing. Overall, the morphology of the pterygoid region is very similar to the morphology of the pterygoid in *Chilcacetus*. The anterior margin of the pterygoid is situated just posterior to the antorbital notch; the pterygoid sinus fossa as a result does not extend anterior to the antorbital notch. The medial contact of the left and right pterygoid is damaged. The medial lamina of the pterygoid forms the lateral wall of the internal nares. The eustachian notch is missing, but it appears that that medial lamina of the pterygoid contributes to the anterior portion of the pharyngeal crest. The lateral lamina of the pterygoid is better preserved on the right side. The lateral lamina is a thin but prominent ridge; and forms the ventromedial edge of the frontal groove. The lateral lamina appears to contact the alisphenoid, but due to damage to the basicranium, it is difficult to confirm this. The lateral lamina does not appear to have contacted the falciform process of the squamosal, differing from the condition seen in platanistids, squalodelphinids, and some eurhinodelphinids. The pterygoid sinus fossa is roughly triangular in shape; the orbit lacks any deep fossae suggesting an orbital lobe of the pterygoid sinus.

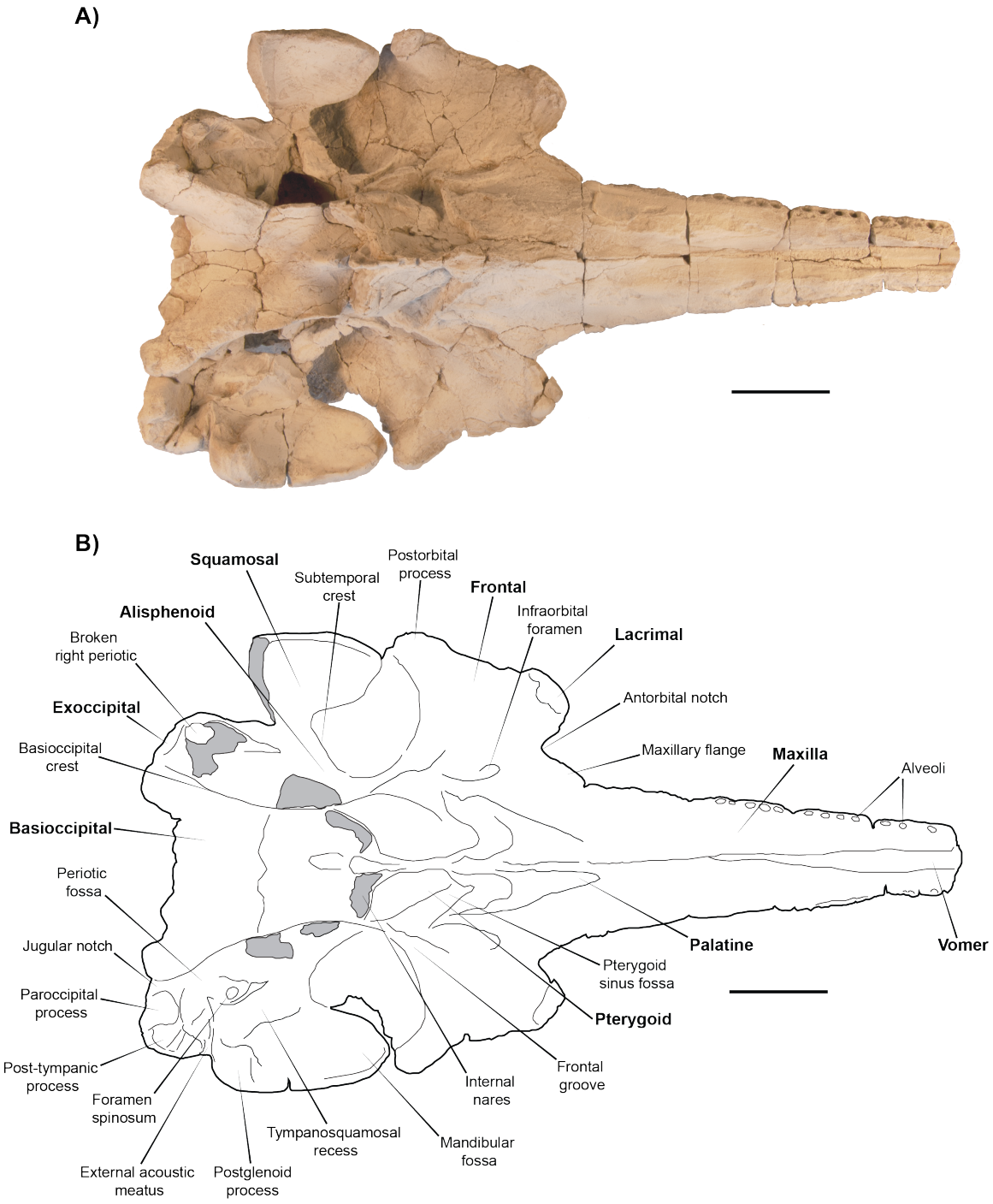

Figure 6 Photo (a) and line drawing (b) of the skull of *Perditicetus yaconensis*, USNM 335224 (holotype), ventral view. The names of bones are in bold type; grey areas indicate either broken surfaces or infilling matrix. Scale bar = 5 cm. Note that the alveoli are subequal in size, indicating single-rooted teeth; also note the wide exposure of the pterygoid and the separation of the periotic fossa into anterior and posterior fossae.

Nasal

The nasals have a medial contact that points anteriorly, giving the external nares a heart-shaped appearance in anterior and dorsal view. This medial contact is shifted to the left of the midline. The left and right nasals are asymmetrical, though this appears to be the result of damage. The anterior edge of the left nasal trends posterolaterally, where it contacts the premaxilla and maxilla. The left nasal appears to slightly overhang the left external naris. There is a trough posterior to the external nares, forming a depression between the nasals and the vertex of the skull. The contact between the nasals and frontals is indistinguishable and likely fused.

Mesethmoid

The mesethmoid clearly forms the dorsal and posterior borders of the narial passages. However, the area directly anterior of the posterior border of the external nares is largely obscured by remaining in-filling matrix. The dorsal portion of the mesethmoid contributes to the anterior projection that gives the external nares its heart-shaped appearance. The ossified nasal septum is a very thin plate of bone, approximately 3 mm thick, extending down to the level of the premaxillary sac fossa.

Vomer

The vomer forms the lining of the mesorostral groove. It is not exposed at all in dorsal view due to infilling matrix and contact between the premaxillae. In ventral view, the vomer is exposed between the maxillae to the level of the posterior alveoli. Its widest ventral exposure measures 11 mm. Posteriorly, the vomer forms the septum that separates

the internal nares. The suture between the vomer and the basioccipital is not distinguishable.

Lacrimal

The lacrimal is poorly defined in dorsal view, due to fusion of the sutures between the lacrimal and the frontal and maxilla on the right. The left lacrimal appears to have been broken and reassembled. In dorsal view, the lacrimal forms the anterior-most part of the antorbital process. In ventral view, a thin portion of the lacrimal may contribute to the antorbital notch. The lacrimal appears to be thick dorsoventrally, and transversely wide. This gives the antorbital process a triangular shape in dorsal and ventral view. The ventral exposures of the lacrimal are broken on both the left and the right side. No remnants of the jugal remains. There does not appear to be a lacrimal groove or foramen.

Frontal

The frontals have a tabular exposure at the vertex where they are fused to the nasals. They likely form part of the transverse trough posterior to the external nares. Moving posterolaterally from the external nares, the frontals appear to "pinch out" between the maxilla and supraoccipital. The frontals likely contribute to the prominent nuchal crest. The frontal forms part of the dorsal surface of the supraorbital process. In lateral view, the postorbital process of the frontal is thickened and triangular in profile. The postorbital process is directed posteroventrally (Fig. 5). Posteriorly, the frontal is indistinguishable from the ascending process of the maxilla in lateral view. In ventral view, the frontal forms the shallow, elongate, and slightly concave orbit. There is a slight preorbital ridge formed from the margin of the lacrimal. The frontal bears a large

infraorbital foramen situated posteromedial to the antorbital notch. Just posterior to the infraorbital foramen is a fossa, likely for the pterygoid sinus. There is a prominent frontal groove, an extension of the optic canal, that likely contacts the orbitosphenoid. This groove likely transmitted the optic nerve. The postorbital ridge forms the posterolateral edge of the frontal groove and appears to contact the alisphenoid. The postorbital ridge is not pronounced. There is no deep fossa in the orbit for an extension of the pterygoid sinus.

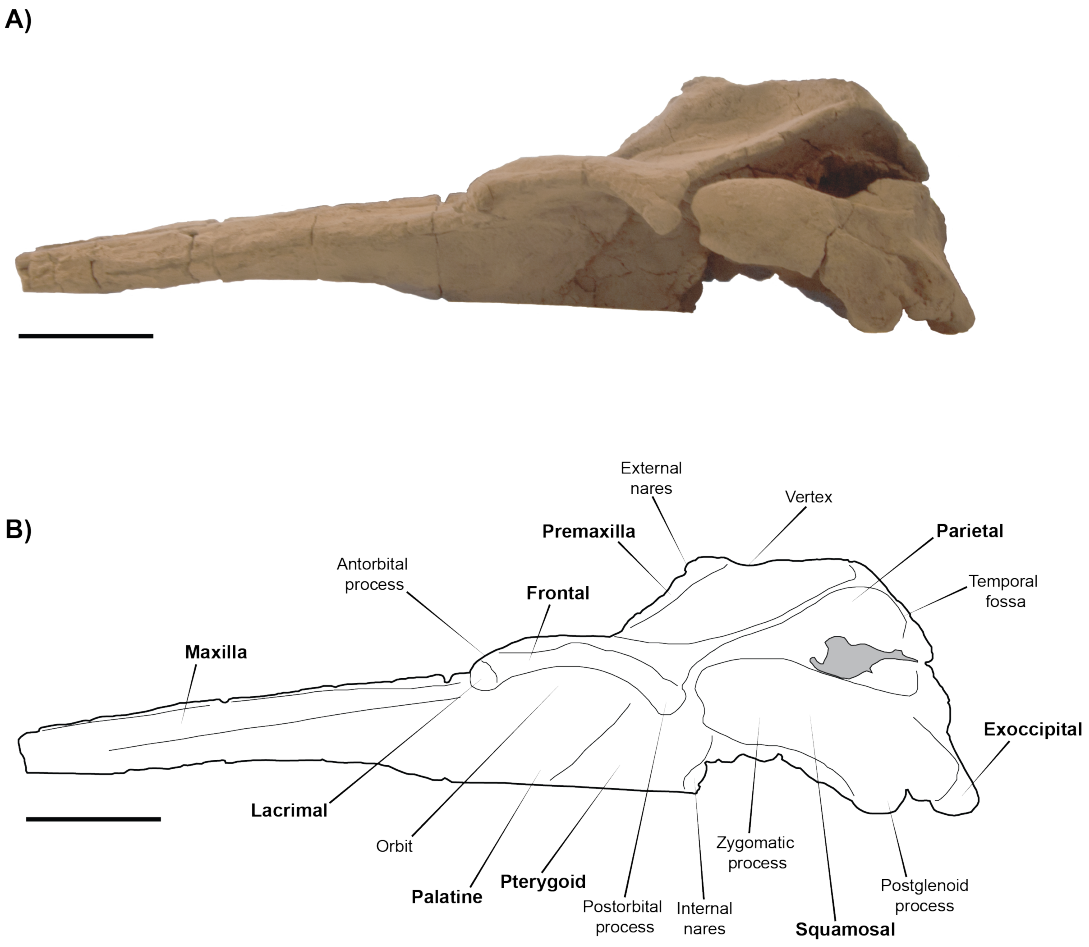

Figure 7 Photo (a) and line drawing (b) of the skull of *Perditicetus yaconensis*, USNM 335224 (holotype), lateral view. The names of bones are in bold type; grey areas indicate either broken surfaces or infilling matrix. Scale bar = 5 cm. Note that the vertex is roughly level with the dorsalmost edge of the temporal fossa, and the dorsoventrally expanded zygomatic process.

Parietal

The parietal does not appear to be exposed at the vertex; if so, it is part of the "pinching out" section described above; and could be part of the nuchal crest. However, due to the level of fusion present in the vertex, it is extremely difficult to distinguish the parietal from the frontal. No interparietal appears to be present. In lateral view, sections of the parietal are broken on both sides, exposing matrix that fills the braincase. Part of the suture between the parietal and squamosal is missing as a result. The parietal forms a thin, but prominent, temporal crest that overhangs the temporal fossa. The parietal forms the medial wall of the temporal fossa, and the braincase appears slightly inflated. The dorsolateral suture between the parietal and the supraoccipitals is fused. In ventral view, the large holes obscure any ventral exposures of the parietal. The dorsolateral contact between the parietal and alisphenoid appears to be fused.

Squamosal

In dorsal view, the zygomatic process is directed anteriorly. The anterior margin of the zygomatic process extends to the level of the external nares, and is separated from the postorbital process of the frontal by approximately 5 mm. The dorsal profile of the zygomatic process is rounded both transversely and anteroposteriorly. Posteriorly, above the level of the postglenoid process, the squamosal bears an emargination for attachment of jaw musculature. This emargination likely contacted the lambdoid crest of the

supraoccipitals. The dorsal surface directly lateral to the braincase bears a depression that forms the floor of the temporal fossa. In both dorsal and lateral view, the zygomatic process is thickened dorsoventrally, similar to the condition seen in squalodelphinids and platanistids. The ventral edge of the zygomatic process is concave in lateral view. There is a prominent, rounded postglenoid process. Despite the damage to the basicranium, the ventral surface of the squamosal on the left side is well-preserved. The zygomatic process has a concave lateral edge but becomes flatter medially. The surface of the mandibular fossa is very smooth; at the anterolateral margin of the zygomatic process, a facet for the jugal is preserved. The tympanosquamosal recess is shallow and weakly separated from the mandibular fossa; there is only a slight ridge separating them. The falciform process is broken off and missing. Based on a broken surface present anteromedially to the external acoustic meatus, I infer that USNM 335224 had a spiny process. The anterior contact between the squamosal and the alisphenoid is indistinct, largely due to damage. Posterior to the broken base of the falciform process, there is a large foramen, tentatively identified as the foramen spinosum (responsible for transmitting the middle meningeal artery). There is a large periotic fossa situated posteriorly. This fossa measures approximately 32 mm from the base of the falciform process to the anterior edge of the exoccipital, and 23 mm transversely from the medial edge of the tympanosquamosal recess to the contact with the basioccipital. The periotic appears to approximate the squamosal at the lateral tuberosity and part of the anterior process. Dorsally, there does not appear to be a large cavity between the periotic fossa and the pars cochlearis. The periotic fossa in the holotype is weakly split into anterior and posterior sections by a

supratubercular ridge (*sensu* Fordyce, 1994). The anterior portion is smaller and is slightly dorsoventrally deeper than the posterior portion. In the posterior portion of the periotic fossa, there appears to be an excavation, partially obscured by matrix, in the wall of the periotic. This is interpreted to be the suprameatal pit of the squamosal; and marks the articulation between the articular rim of the periotic and the squamosal. The external acoustic meatus opens medially just dorsal to the base of the spiny process. It is narrow medially but widens laterally; and is bounded by anterior and posterior meatal crests. The anterior meatal crest is partially broken but extended from the postglenoid process to the base of the spiny process. The posterior meatal crest separates the external acoustic meatus from the post-tympanic process. There are two sutures present in the post-tympanic process where the posterior process of the tympanic bulla contacts the squamosal.

Supraoccipital

The supraoccipital is framed by the nuchal crest, which is somewhat convex anteriorly. The nuchal crest is prominent, elevated 10-12 mm above the ascending process of the maxilla. The occipital shield is smoothly concave, forming a medial depression in the supraoccipitals (Fig. 6). The posterior-most portion of the supraoccipitals is missing or broken, due to the absence of the occipital condyles. As a result, the contact between the supraoccipital and the exoccipitals is missing. Due to the damage on the lateral portions of the skull, the contact with the squamosal is also missing.

Basioccipital

In ventral view, the contact between the basioccipital and vomer appears to be fused. The basioccipital crests are long and prominent, and run about half the length of the basicranium. The basioccipital crests are indistinguishable from the pharyngeal crests. Transversely the crests are robust but possess a thin ventral margin. Anteriorly, the basioccipital crests are roughly parallel but begin to diverge at the level of the foramen ovale/cranial hiatus. In the medial basioccipital there is a deep depression. The carotid foramen is not visible.

Exoccipital

The right exoccipital is largely missing and heavily damaged; the portion surrounding the missing occipital condyles is also damaged. Due to this damage, the contact between the exoccipitals and supraoccipital is missing. However, the left exoccipital is otherwise well-preserved. The posterior surface of the exoccipital is flat to gently concave. The dorsal contact between the exoccipital and the parietal appears fused. Ventrally, the exoccipital forms the posterior-most portion of the basioccipital crest, directly medial to the deep jugular foramen, which transmits the glossopharyngeal, vagus, and accessory nerves. The hypoglossal foramen is not apparent. The paroccipital process is robust, with prominent sutures for the tympanic bulla. There does not appear to be a distinct fossa for the posterior sinus. Laterally, the contact between the exoccipital and the post-tympanic process of the squamosal is fused.

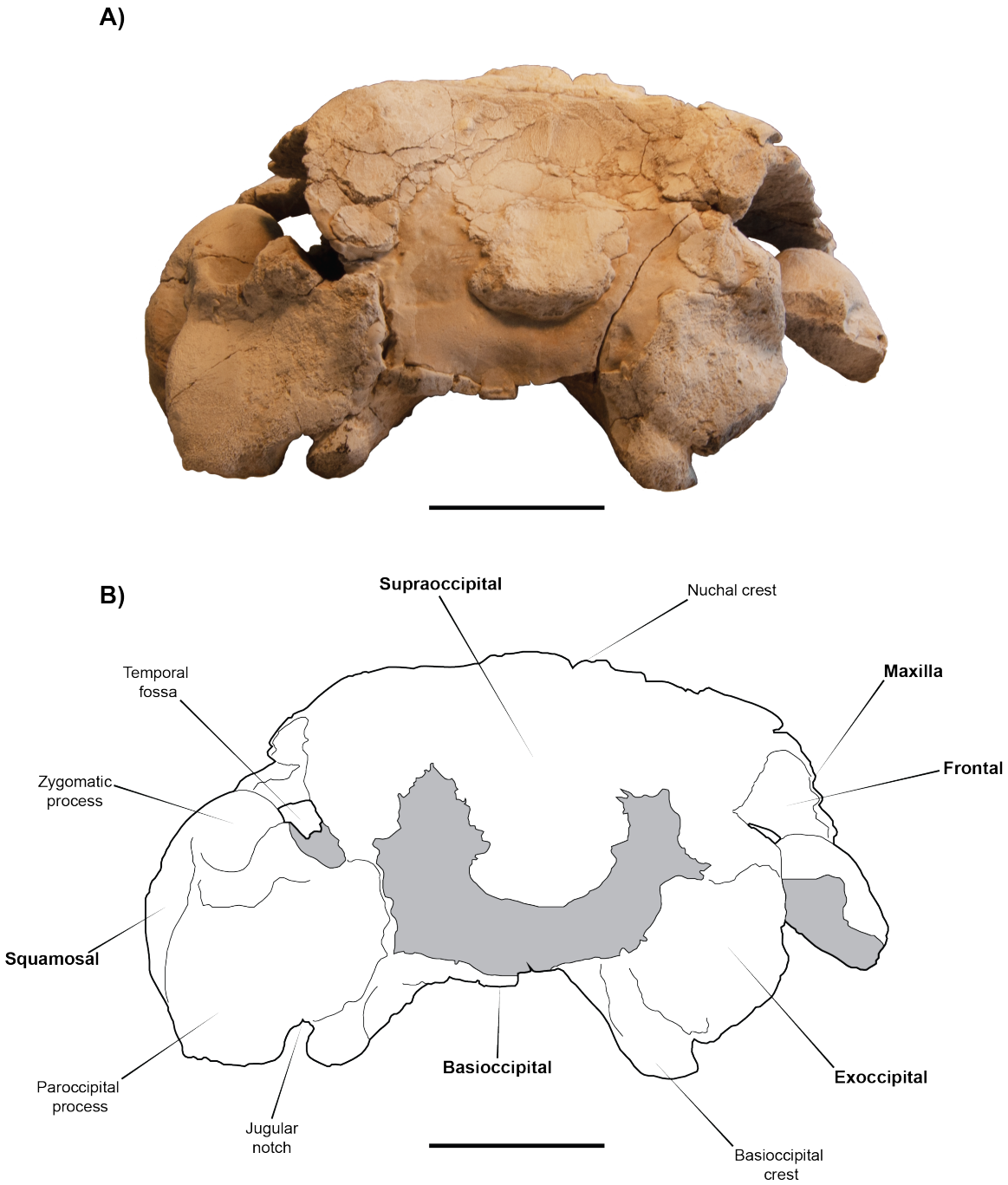

Figure 8 Photo (a) and line drawing (b) of the skull of *Perditicetus yaconensis*, USNM 335224 (holotype), posterior view. The names of bones are in bold type; grey areas indicate either broken surfaces or infilling matrix. Scale bar = 5 cm. Note the emargination of the squamosal and exoccipital for neck muscle fossae in the temporal fossa.

Alisphenoid, basisphenoid, orbitosphenoid

The alisphenoid is the only portion of the sphenoid bone that can be distinguished in the holotype. In ventral view, the alisphenoid contributes to the subtemporal crest. It does not appear to contribute to the pterygoid sinus fossa. Due to the damage to the basicranium, the position of the foramen ovale and the orbital fissure cannot be determined. There is no clear sphenoidal suture between the alisphenoid and the squamosal. The basisphenoid appears to be covered by the vomer, and the carotid foramen is obscured. The orbitosphenoid is indistinct.

Table 1 Measurements of the skull of *Perditicetus yaconensis*, USNM 335224, holotype (mm). Measurements from Fordyce (1994).

Condylobasal length	>378
Rostrum length	>207
Rostrum width at base	97
Rostrum width at preserved mid length	59
Premaxillary width dorsally at level of antorbital notches	45
Maximum premaxillary width dorsally, about level with mid-orbit	65
Distance from level of antorbital notches to most anterior border of nasals	86
Distance from level of antorbital notches to border of internal nares	80
Cranial length	>186
Preorbital width at level of lacrimal-frontal suture	176
Postorbital width, maximum across postorbital processes	218
Palatine length, in midline	116
Maximum width of external nares	31
Width of left frontal at level of apex of premaxilla	25
Width of right frontal at level of apex of premaxilla	26
Minimum width, intertemporal constriction	75
Distance from anterior of inter-nasal suture to apex of supraoccipital	50
Maximum width across zygomatic processes	225
Point-to-point distance, apex of supraoccipital to dorsal intercondylar notch	-

Periotic (left)

The left periotic of the holotype is well preserved; the right periotic partially remains in the periotic fossa and partially attached to the tympanic bulla. The periotic, as viewed dorsally, has a sigmoidal profile. The length of the anterior process of the periotic is long, being greater than 60% the length of the pars cochlearis. There is a dorsal tubercle present on the anterior process (Fig. 7a-b). The apex of the anterior process is rounded. Viewed ventrally, there is one thin anterointernal sulcus, associated with the dorsal tubercle (Fig. 7c-d). In lateral view, the axis of the anterior process is angled downwards (Fig 7e-f). The anterior keel, as well as the anteroventral angle, are indistinct. The anterior bullar facet is well preserved and forms a deep depression; this condition is similar to that seen in eurhinodelphinids, squalodelphinids, and platanistids. The periotic does not have a parabullary ridge. The fovea epitubaria, posterior to the anterior bullar facet, is long and deep, similar to the condition seen in *Notocetus*. Lateral to the anterior bullar facet and the fovea epitubaria is a weakly curved anteroexternal sulcus (called the parabullary sulcus in other publications). The periotic has a small groove, interpreted as the fossa for the tegmen tympani muscle, medial to the mallear fossa. The pars cochlearis is somewhat inflated; the profile is semispherical as opposed to square. The fenestra rotunda is subrounded ventrally; it appears to be connected to the aperture for the cochlear aqueduct via a fissure. Dorsally, there is a faint rim that surrounds the pyriform internal acoustic meatus. Internally, the internal acoustic meatus is filled with matrix. The aperture for the cochlear aqueduct opens dorsomedially and is approximately the same size as the aperture for the vestibular aqueduct. The dorsal surface appears to have a

ridge, giving the periotic its sigmoidal profile, but the dorsal tuberosity on the anterior process and the articular rim on the posterior process may account for this ridge; the periotic would not have a dorsal crest like that seen in *Waipatia*. There is no superior petrosal sinus or subarcuate fossa visible. There is a shallow lateral groove dorsal to the lateral tuberosity. Ventrally, the lateral tuberosity is large and blunt; the apparent separation between the lateral margin of the anterior process and the lateral tuberosity appears to be artificial. The hiatus epitympanicus is wide and concave; in ventral view, it appears to be narrow medially. The mallear fossa lies medial to the lateral tuberosity and is bowl-shaped. The fenestra ovalis is subcircular and is situated dorsal to the ventral surface of the pars cochlearis. The ventral foramen for the facial canal is situated directly lateral to the fenestra ovalis; the sulcus for the facial nerve is not visible. The stapedial muscle fossa is obscured by infilling matrix. The posterior process and pars cochlearis are subequal in length. Like the anterior process, the posterior process of the periotic is bent ventrally in medial and lateral view. The posterior bullar facet is wide and roughly fan-shaped, being wider posteriorly than it is anteriorly. The ventral surface of the posterior bullar facet is very smooth. The posteroexternal foramen is not visible. Notably, the periotic of USNM 335224 possesses a small articular rim on the lateral face of the posterior process (Fig. 7g-h). The articular rim in *Perditicetus* is less developed than that seen in *Huaridelphis* and *Notocetus* but is more developed than the "incipient articular rim" of *Waipatia* (Fordyce, 1994).

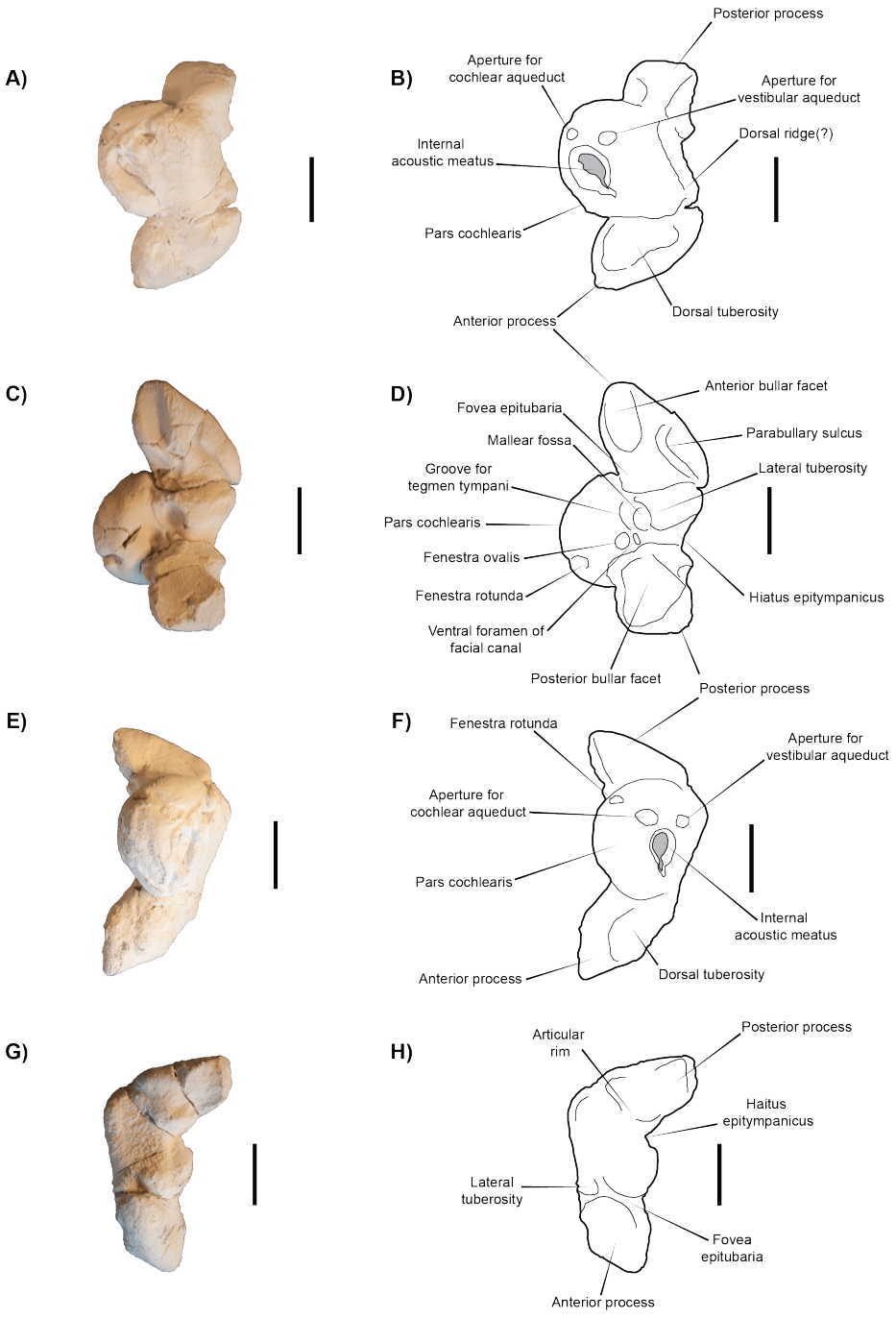

Figure 9 Photo (a) and line drawing (b) of the left periotic of *Perditicetus yaconensis*, USNM 335224 (holotype), dorsal view; photo (c) and line drawing (d) of the periotic, ventral view; photo (e) and line drawing (f) of the periotic, medial view; photo (g) and line drawing (h) of the periotic, lateral view. Grey areas indicate either broken surfaces or infilling matrix. Scale bar = 1 cm. Note the weakly curved parabullary sulcus in ventral view and the articular rim visible in lateral view.

Table 2 Measurements of the left periotic of *Perditicetus yaconensis*, USNM 335224, holotype (mm). Measurements from Fordyce (1994).

Anteroposterior length	36
Width, internal margin of pars cochlearis to external margin at hiatus epitympanicus, level with fenestra ovalis	18
Length of pars cochlearis, from groove for tensor tympani to mid-point of stapedial muscle fossa	15
Length of internal auditory meatus	5
Length of posterior bullar facet	10

Tympanic Bulla (right)

The right tympanic bulla is poorly preserved. A portion of the right periotic (likely the pars cochlearis) appears to still be attached to the broken posterior process or to the tympanic bulla itself (Fig. 8a-b). The tympanic bulla is roughly square shaped, being subequal length and width. The involucrum is present, as well as the inner posterior prominence. There are several striae on the dorsal surface of the involucrum, though these could possibly be tool marks. The sigmoid process, as well as any accessory ossicle, is also missing. It appears that the entire ventral side has broken off, leaving only fragments of internal bone with matrix filling the tympanic cavity (Fig. 8c-d). The tympanic bulla, when articulated with the skull, takes up much of the periotic fossa, suggesting that *Perditicetus* possessed a small peribullary sinus.

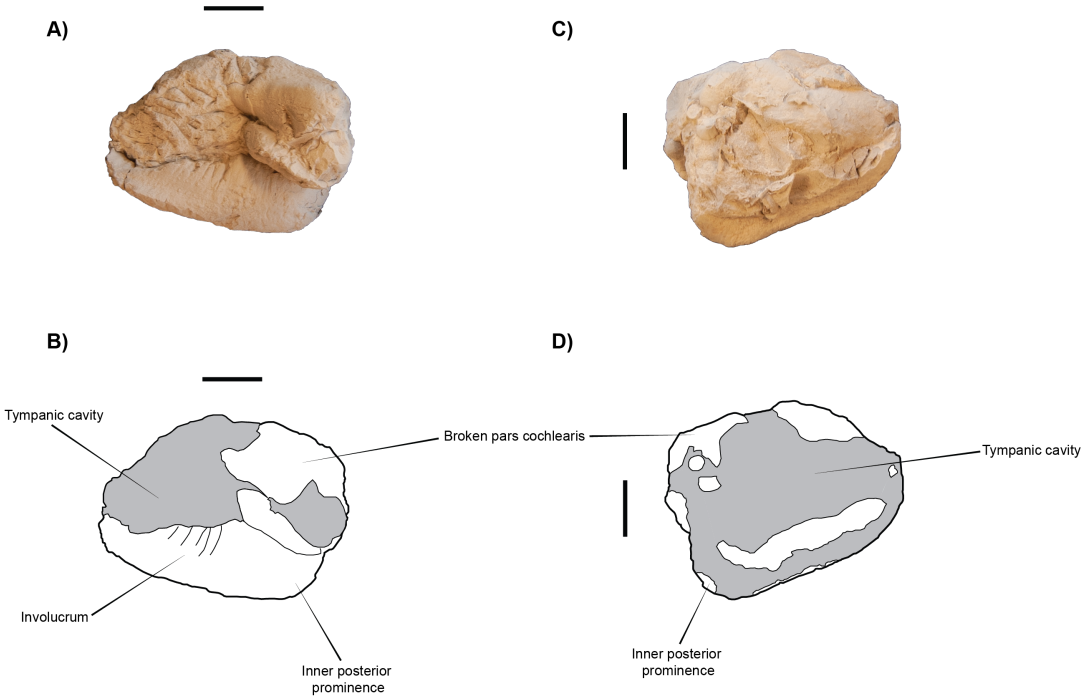

Figure 10 Photo (a) and line drawing (b) of the right tympanic bulla of *Perditicetus yaconensis*, USNM 335224 (holotype), dorsal view; photo (c) and line drawing (d) of the tympanic bulla, ventral view. Grey areas indicate either broken surfaces or infilling matrix. Scale bar = 1 cm.

Table 3 Measurements of the right tympanic bulla of *Perditicetus yaconensis*, USNM 335224, holotype (mm). Measurements from Fordyce (1994).

Standard length, anterior apex to apex of outer posterior prominence	-
Length, anterior apex to apex of inner posterior prominence	38
Distance, outer posterior prominence to apex of sigmoid process	-
Dorsoventral depth of involucrum immediately in front of posterior pedicle	12
Elliptical foramen	-
Maximum point-to-point length of posterior process	-

DISCUSSION

Morphology, Homology, and Function

Here, I briefly discuss structures noted in the description, their morphology, and the function of these structures. Several soft tissues, such as musculature, the air sinus system, and sensory organs have osteological correlates; thus, I can make some inferences of the soft tissue structures present in *Perditicetus*. Regarding facial structure, *Perditicetus* is more derived than stem odontocetes such as *Agorophius* in that the facial bones are more telescoped such that the vertex of the skull has shifted more posteriorly, in the roofing over of the temporal fossa by the maxilla and frontal, and no prominent intertemporal constriction. As seen in many odontocetes, *Perditicetus* displays some asymmetry of the facial region; the asymmetry of the facial bones reflects asymmetry in the overlying facial muscles, such as the masillonasiolabialis muscle. The purpose of the asymmetry of the bones and soft structures is still debated, but sound production is a strong explanation (Cranford et al., 1996; Fahlke and Hampe, 2015).

The facial structure of odontocetes is highly specialized for echolocation: they possess a system of nasal air sacs and fat bodies that aid in sound production and isolation. Of these features, several leave osteological correlates. First, the premaxillary sac, one of the nasal air sacs used to acoustically isolate the phonic lips and to act as reservoirs for air required for sound production (Cranford et al., 1996), contacts the

dorsal surface of the rostrum. This forms the premaxillary sac fossa, which is present in the holotype of *Perditicetus*. Second, modern odontocetes have a body of fat and connective tissue known as the melon, likely used to focus vocalizations (McKenna et al., 2012). The melon corresponds to the concave facial region seen in almost all odontocetes, including *Perditicetus*. In the mandible of odontocetes, there is a fat pad present associated with a large mandibular foramen (Cranford et al., 2010). As the mandible is missing in the holotype, the presence of a fat pad cannot be confirmed for *Perditicetus*. However, based on the other two structures are present in the holotype, and considering that stem odontocetes such as *Cotylocara* display such osteological correlates, *Perditicetus* was almost certainly capable of echolocating.

Feeding ecologies in cetaceans can be assessed based on the length of the rostrum and the teeth present. Like extant odontocetes, *Perditicetus* was polydont and most likely homodont. Since homodonty reflects a decrease in mastication (Loch and Simoes-Lopes, 2013), it is likely that *Perditicetus* did not do any significant oral processing of food; however, teeth in another specimen of this genus would be required to confirm this. *Perditicetus* was moderately longirostral, with a rostrum length at least 55% of the condylobasal length and considering that the apex of the rostrum is missing in the holotype, the full length of the rostrum could be longer. Extant longirostral odontocetes *Platanista* and *Inia*, both river dolphins, feed by raptorial snapping (Werth, 2000). It is likely that *Perditicetus* was also a snap raptorial feeder. This feeding ecology was prevalent in many Oligocene and Miocene odontocete taxa, but is now entirely confined to the “river dolphins” inhabiting freshwater environments (McCurry and Pyenson,

2018). Fordyce (1994) notes that the long lateral lamina of the pterygoid that contacts the falciform process, such as the one seen in the hyper-longirostral eurhinodelphinids and platanistids, could be origin of the internal pterygoid muscle; this feature is missing in *Perditicetus*.

The tympanoperiotic complex in cetaceans has been heavily modified to enable them to hear in water, such as the presence of a pachyosteosclerotic tympanic bulla (Luo and Gingerich, 1999). In odontocetes, the bones of the ear have been further modified in order to echolocate. In many odontocetes, the ear bones are separated from the rest of the basicranium, due to the formation of a cranial hiatus and the air sinus system; the cranial hiatus in *Perditicetus* appears to be missing, possibly closed during ontogeny (Mead and Fordyce, 2009). Structures related to hearing in *Perditicetus* include the fenestra ovalis, through which the stapes makes contact with the inner ear. The semispherical pars cochlearis houses the inner ear. On the dorsal surface of the pars cochlearis, the internal acoustic meatus transmits the vestibulocochlear nerve, which is responsible for hearing and balance (Ekdale and Racicot, 2015; Spoor et al., 2002). *Perditicetus*, like other platanistoids, possesses an articular rim, which contacts the suprameatal pit of the squamosal. In the platanistids *Pomatodelphis*, *Zarhachis*, and *Platanista*, the articular rim is developed into the hook-like articular process, which creates an interlocking contact between periotic and squamosal (de Muizon, 1987). The purpose of the articular rim or articular process remains unknown. The articular rim seen in platanistoids differs from a small articular “peg” or tubercle seen in eurhinodelphinids, *Chilcacetus*, and possibly *Waipatia*. This feature is often referred to as an “incipient articular rim” (Fordyce, 1994)

but de Muizon (1987) suggests this tubercle is a vestigial articulation between periotic and squamosal.

The extensive accessory sinus system is a hallmark of odontocetes; these sinuses are air-filled and heavily vascularized, and act to acoustically isolate the ear bones from the basicranium (Costidis and Rommel, 2012; Fraser and Purves, 1960). In *Perditicetus*, the most noticeable of these accessory sinuses' osteological correlates is the pterygoid sinus fossa. This fossa is bounded by the anterior extent of the pterygoid, and the medial and lateral laminae of the pterygoid. Unlike *Waipatia*, *Perditicetus* does not appear to have a fossa in the alisphenoid/basisphenoid for the pterygoid sinus fossa (Fordyce, 1994). *Perditicetus* differs from other derived platanistoids by lacking an orbital fossa for the pterygoid sinus. Bony fossae only record the minimum extent of the sinus system, so that absence of a fossa does not indicate absence of an accessory sinus. Unlike more derived taxa such as the delphinids, the holotype lacks an anterior sinus fossa. The middle sinus occupies the area surrounding the mandibular fossa and postglenoid process; the tympanosquamosal recess is considered an osteological correlate (Mead and Fordyce, 2009). The tympanosquamosal recess is shallow but present in the holotype, indicating that *Perditicetus* possessed a middle sinus. The tympanic bulla and the periotic are not separated from the squamosal by a large cavity, indicating a modestly sized peribullary and posterior sinus.

Cladistic Relationships

As stated under the Materials and Methods section, I carried out three phylogenetic analyses: the phylogenetic analysis (Analysis 1) in the publication of

Arktocara was the largest, encompassing the greatest variation in taxa (Boersma and Pyenson, 2016); the analysis (Analysis 2) in the publication of *Dilophodelphis*, which focused almost entirely on relationships between platanistoids (Boersma et al, 2017); and the analysis (Analysis 3) in the publication of *Chilcacetus*, which included a wider variety of basal crown odontocetes (Lambert et al, 2015). All three analyses placed *Perditicetus* within the Platanistoidea. I will discuss the results of each analysis below.

After running Analysis 1, I retained 320,112 most parsimonious trees, with a score of 1984 steps. The strict consensus (Fig. 9) and majority rule consensus (Fig. 10) are shown below. The strict consensus tree is poorly defined, with much of the Odontoceti forming a polytomy. In the strict consensus, the Platanistoidea, defined as Allodelphinidae + Squalodelphinidae + Platanistidae, is polyphyletic, with the Squalodelphinidae and Platanistidae being sister taxa to each other. In the majority rule consensus, I recover a monophyletic Platanistoidea *sensu* Lambert et al. (2014), as well as a monophyletic Platanistidae and Allodelphinidae. However, I do not recover a monophyletic Squalodelphinidae. The historically considered platanistoids, *Squalodon* and the Waipatiidae, appear as stem Odontoceti. Characters that place *Perditicetus* in the Platanistoidea include: the articular rim of the periotic, the weakly curved parabullary sulcus, the sigmoidal profile of the periotic, and an anteroposterior ridge on the dorsal side of the periotic. The reason why *Perditicetus* allies with the Allodelphinidae in this analysis is unclear; there are no synapomorphies uniting *Perditicetus* + Allodelphinidae. For this reason, I still consider *Perditicetus* to be family *incertae sedis*.

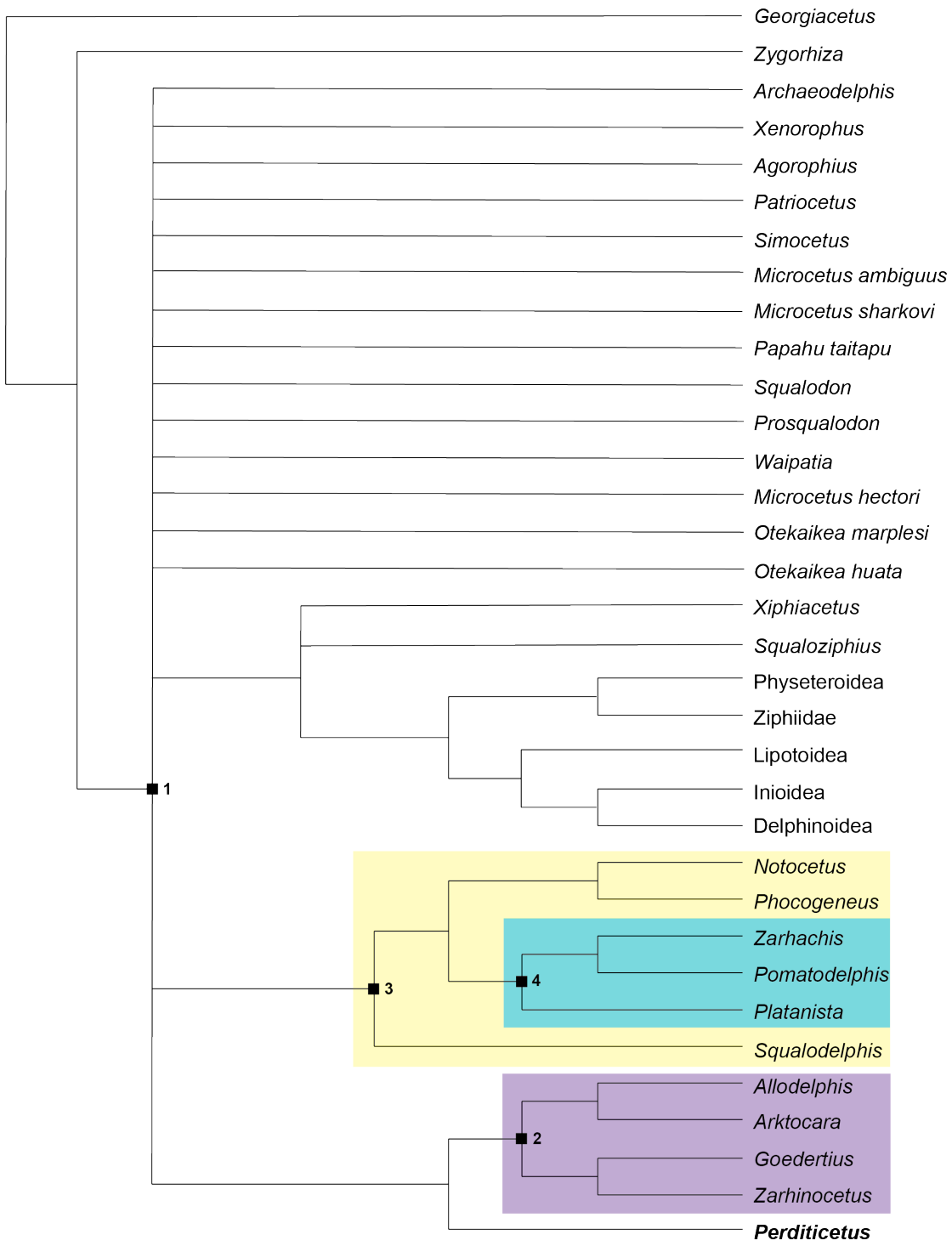

Figure 11 Strict consensus phylogeny of Analysis 1 (Boersma and Pyenson 2016). Bold numbers at nodes indicate the following clades: 1) Odontoceti, 2) Allodelphinidae, 3) "Squalodelphinidae" + Platanistidae. Note the poor resolution of Odontoceti, resulting in a large polytomy.

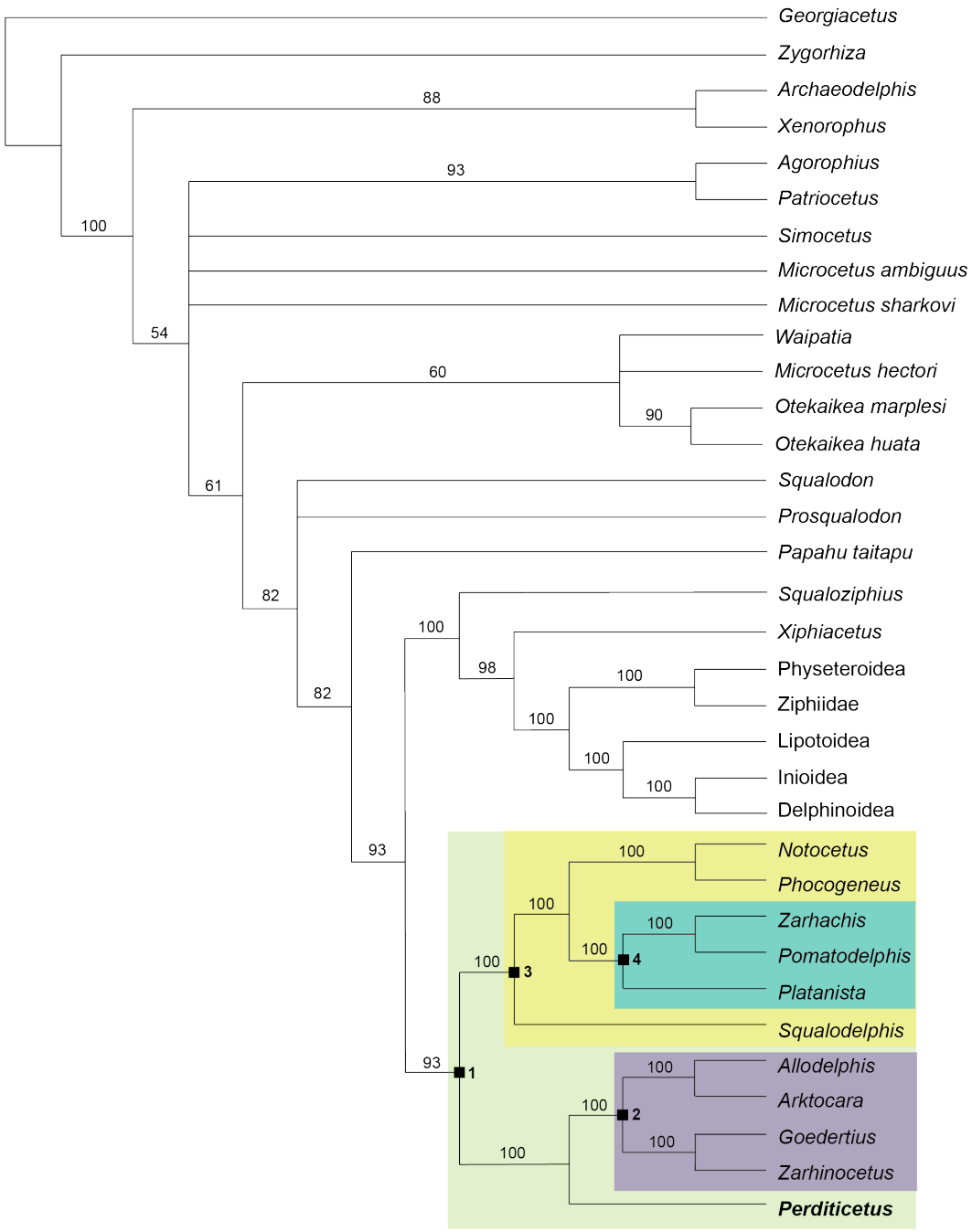

Figure 12 50% majority rule consensus of Analysis 1 (Boersma and Pyenson, 2016). Numbers over branches indicate the percent of occurrence over all most parsimonious trees. Bold numbers at nodes indicate the following clades: 1) Platanistoidea;2) Allodelphinidae; 3) Squalodelphinidae + Platanistidae; 4) Platanistidae.

Analysis 2 was the most limited of the three analyses, with all but two taxa considered platanistoids by various authors. I obtained 14 most parsimonious trees with 157 steps (Fig. 11-12). This analysis placed *Perditicetus* as the sister taxon to the Platanistoidea as defined Allodelphinidae + Squalodelphinidae + Platanistidae in the strict consensus tree; this analysis also resolved monophyly for the Allodelphinidae, Squalodelphinidae, and Platanistidae, but a paraphyletic Waipatiidae. However, without any more derived taxa (such as ziphiids or delphinoids) it is difficult to rely on the results of this analysis. The node for the Platanistoidea could be drawn several places depending on the philosophy of the author. Characters in this analysis that align *Perditicetus* with the clade Allodelphinidae + Squalodelphinidae + Platanistidae are: widening of the cranium and loss of double-rooted teeth. When a broader concept of the Platanistoidea is applied, in which I include waipatiids and *Squalodon* as platanistoids, characters that place *Perditicetus* in the Platanistoidea are: emargination of posterior edge of zygomatic process by fossa for neck musculature, the presence of a foramen spinosum, a posterior portion of the periotic fossa, a lateral groove or depression of the periotic, a parabullary sulcus, and an articular rim of the periotic.

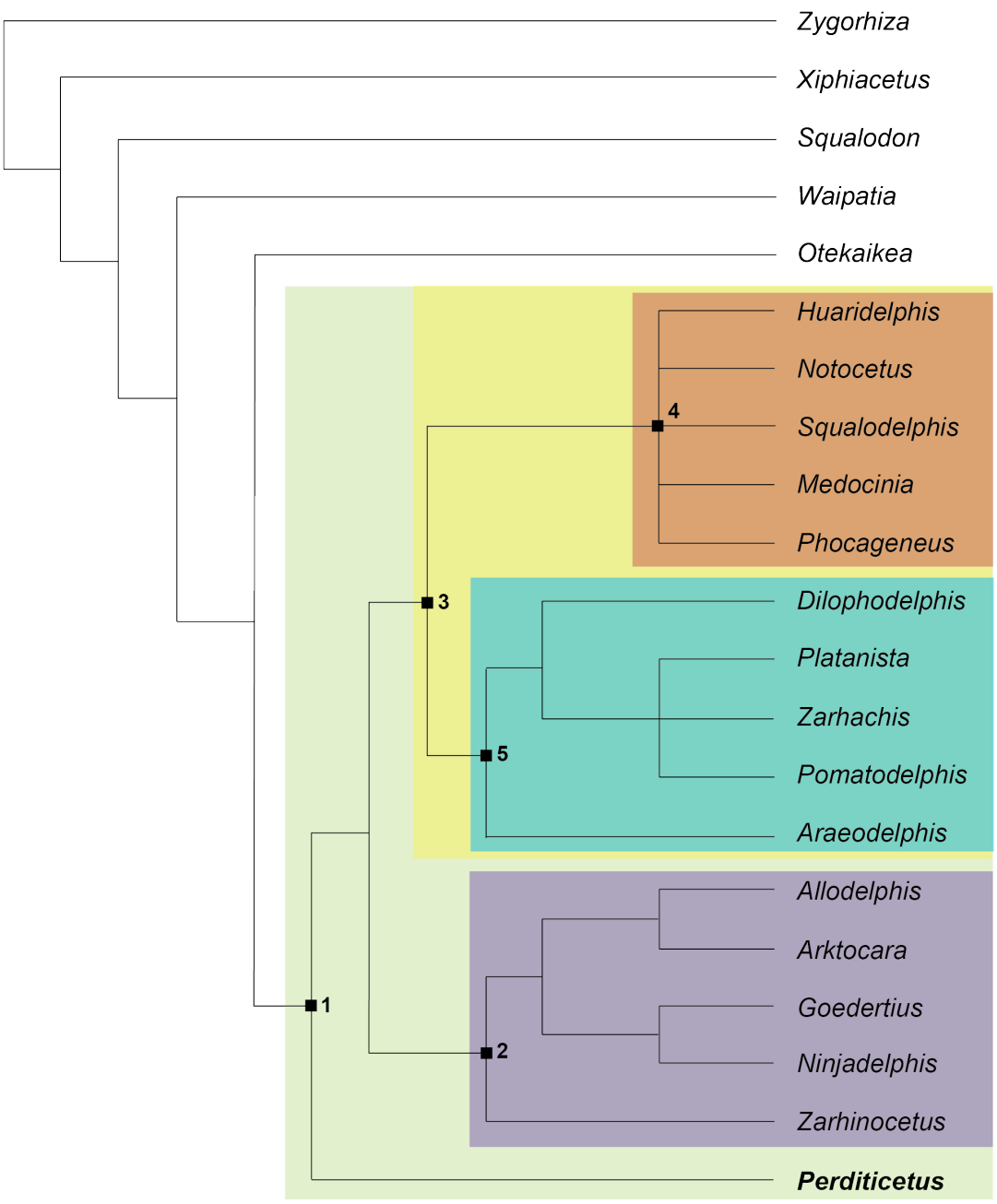

Figure 13 Strict consensus phylogeny of Analysis 2 (Boersma et al., 2017). Bold numbers at nodes indicate the following clades: 1) Platanistoidea *sensu* Lambert et al. (2014); 2) Allodelphinidae; 3) Squalodelphinidae + Platanistidae; 4) Squalodelphinidae; 5) Platanistidae.

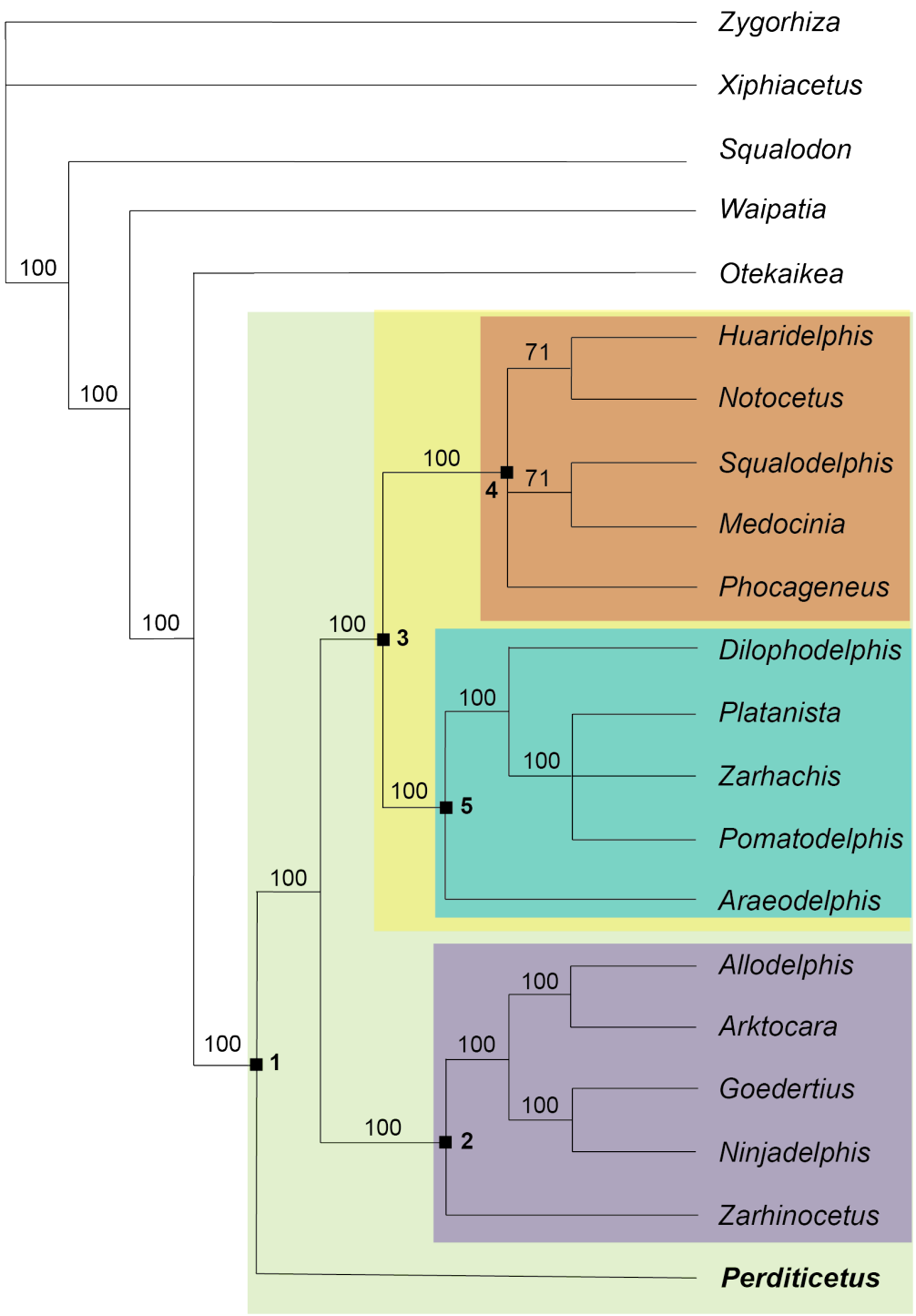

Figure 14 50% majority rule consensus of Analysis 2 (Boersma et al., 2017). Numbers over branches indicate the percent of occurrence over all most parsimonious trees. Bold numbers at nodes indicate the following clades: 1) Platanistoidea *sensu* Lambert et al. (2014); 2) Allodelphinidae; 3) Squalodelphinidae + Platanistidae; 4) Squalodelphinidae; 5) Platanistidae.

Lastly, Analysis 3 (Fig. 13) is intriguing as it contains other basal crown odontocetes not frequently included in other phylogenetic analyses. I obtained 18 most parsimonious trees with 235 steps. The strict consensus and 50% majority rule consensus trees were identical. As expanded on under Materials and Methods, this analysis relied on down-weighting homoplastic characters. When I performed the analysis without down-weighting, I obtained poorly-resolved most parsimonious trees. In addition, bootstrap support values reported by Lambert et al. (2015) indicate that adding or removing a taxon could greatly affect the outcome. When *Perditicetus* was included in Analysis 3, I obtained a polyphyletic Platanistoidea; Squalodelphinidae + Platanistidae remained a monophyletic clade with *Perditicetus* as its sister taxon, however the allodelphinids included in this analysis formed a monophyletic clade with the Eurhinodelphinidae. The "*Chilcacetus* clade" as defined by Lambert et al. (2015) was preserved when *Perditicetus* was included, a surprising result when considering similarities between *Chilcacetus* and *Perditicetus*. Characters allying *Perditicetus* with the clade Squalodelphinidae + Platanistidae include: thickening of the zygomatic process of the squamosal and presence of the articular rim of the periotic. The only character that *Perditicetus* shares with the "*Chilcacetus* clade" is the anterior margin of the nasals overhangs the external nares (also shared by *Waipatia*). It is worth noticing that the *Chilcacetus* analysis was limited in the number of characters used (77), and that the characters in the analysis may not capture similarities between taxa.

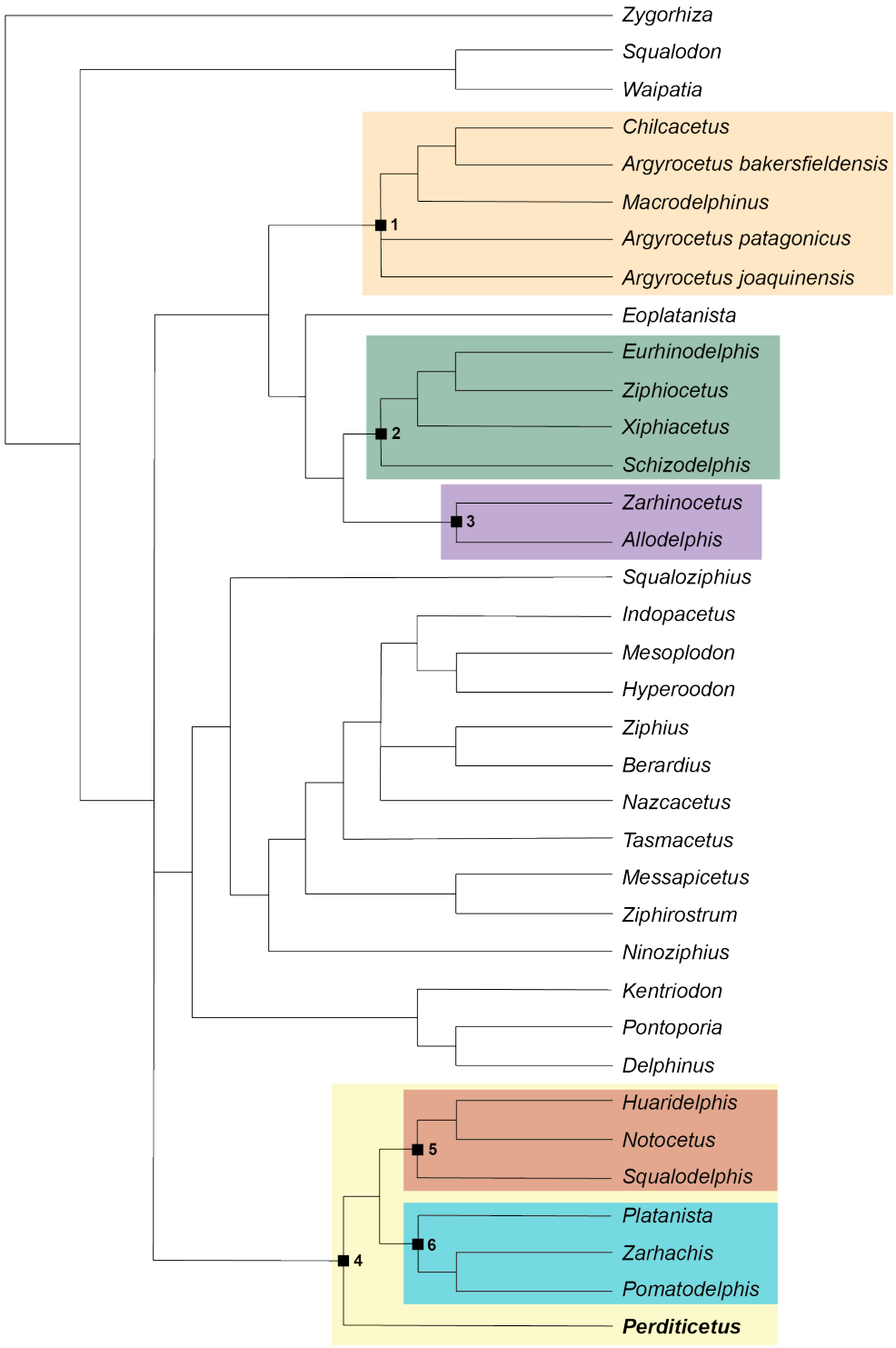

Figure 15 Strict consensus of Analysis 3 (Lambert et al., 2015). Bold numbers at nodes indicate the following clades: 1) "*Chilcacetus* clade"; 2) Eurhinodelphinidae; 3) Allodelphinidae; 4) Squalodelphinidae + Platanistidae +*Perditicetus*; 5) Squalodelphinidae; 6) Platanistidae.

Comparisons to Basal Crown Odontocetes

The skull of *Perditicetus* bears similarity to *Chilcacetus* in multiple regards. In dorsal view, they share a similar morphology of the mesorostral canal, the tabular exposure of nasals and frontals at the vertex, and the lateral extent of the ascending process of the maxilla. In lateral view, their profiles are quite similar: the vertex is at the level of the postorbital process, the nuchal crest and the dorsal-most margin of the temporal fossa are approximately level. and they share a similar morphology of the orbit; they differ in that in *Perditicetus* the supraorbital process is elevated as to obscure part of the ascending processes of the premaxilla and maxilla. The most noticeable difference between *Chilcacetus* and *Perditicetus* in lateral view is that the temporal fossa is smaller and more triangular in shape, and the zygomatic process is far more dorsoventrally and mediolaterally expanded. The morphology of the temporal fossa bears similarity to squalodelphinids and platanistids, who also have dorsoventrally expanded zygomatic processes; this condition is also seen in eurhinodelphinids. However, their vertices are also more elevated than that of *Perditicetus*. In ventral view, *Perditicetus* bears little similarity in the palatine-pterygoid region to allodelphinids, squalodelphinids, platanistids, and some eurhinodelphinids. In these taxa, there is a long lateral lamina of the pterygoid that contacts the falciform process; in *Chilcacetus* and *Perditicetus*, the lateral laminae do not contact the falciform process. *Chilcacetus* and *Perditicetus* also exhibit a separation of the left and right palatines by the maxillae.

However, in the posterior basicranial region, the morphology of *Perditicetus* allies it strongly with the Platanistoidea, as opposed to the "*Chilcacetus* clade". *Perditicetus*, like other platanistoids, exhibits the division of the periotic fossa into anterior and posterior regions. *Perditicetus* also has the suprameatal pit for the contact of the articular rim with the squamosal. And most noticeably, the periotic's morphology, especially the presence of the articular rim, strongly allies it with other platanistoids. In addition, it bears the following similarities to platanistoid periotics: the weakly curved parabullary sulcus, the large anterior bullar facet, the sigmoidal profile of the periotic, and the flat, square-shaped posterior bullar facet. The morphology of the periotic of *Perditicetus* differs greatly from the illustrations of the lost periotic of *Chilcacetus*. *Chilcacetus* lacks an articular rim, the sigmoidal profile, and the curved parabullary sulcus. It is possible that, given that the "*Chilcacetus* clade" is largely supported by symplesiomorphies, similarity between members of the "*Chilcacetus* clade" and *Perditicetus* could be due to homoplasy. This is especially true if *Perditicetus* is truly one of the basalmost platanistoids known, a conclusion that is supported by the results of Analyses 1 and 2. I would suggest that addition of new characters into the phylogenetic analysis of Lambert et al. (2015) could further elucidate the relationship between taxa in the "*Chilcacetus* clade" and *Perditicetus*.

Consistently in phylogenetic analysis, the presence of the articular rim is key in placing *Perditicetus* in the Platanistoidea. Synapomorphies of this superfamily, as described in the Introduction, are incredibly elusive and largely depend on the results of phylogenetic analyses. The initial synapomorphies listed by de Muizon (1987) are

problematic, as the scapula is not a commonly preserved element; I would contend that it is unwise to base a clade's only synapomorphies on an element infrequently preserved in many holotypes. Since the publication of *Huaridelphis* by Lambert et al. (2014), the articular rim of the periotic as emerged as a strong synapomorphy of Platanistoidea. The articular rim, however, is a difficult character to understand, partially as its purpose (if any) is poorly understood, and authors have differing views on what is considered an articular rim. Fordyce (1994) in his publication of *Waipatia* stated that a bulge on the lateral face of the posterior process of the periotic was an "incipient articular rim". However, de Muizon (1987) states that the articular process should not be confused with an "articular peg" that is present in some eurhinodelphinids, which he states is an atavistic articulation between periotic and squamosal. Furthermore, he asserts that specimens of *Zarhachis*, a platanistid with a hook-like articular rim, will exhibit both features on the same periotic. More work is required to fully understand the homology, if any, between Fordyce's "incipient articular rim" and the articular rim of allodelphinids, squalodelphinids, and platanistids. If these features are indeed homologous, this would indicate that single-rooted teeth arose twice in the odontocete lineage; once from the Waipatiidae to more derived members of the Platanistoidea, and again somewhere in stem Odontoceti. If we consider the articular rim as the key synapomorphy of the Platanistoidea, then the Squalodontidae should not be placed in the Platanistoidea, as they lack the articular rim.

Age Considerations

Oligocene platanistoids include *Arktocara*, which is Chattian in age (Boersma and Pyenson 2016), and *Allodelphis pratti*. Squalodontids were abundant during the Chattian and make up the majority of occurrences seen in Figure 16. In addition to *Arktocara* and *A. pratti*, there is also the waipatiid-like *Urkudelphis chawpipacha*, a stem platanistoid from Ecuador, also Chattian in age (Tanaka et al., 2017). Tanaka and Fordyce (2017) describe *Awamokoa tokarahi*, a waipatiid-like odontocete from the late Oligocene of New Zealand, that they placed within the Platanistoidea. Tanaka and Fordyce (2016) argue that *Awamokoa* is possibly the earliest known platanistoid, following the definition of the Platanistoidea outlined in Tanaka and Fordyce (2015b), which includes the Waipatiidae. Despite the fact that the allodelphinid *Goedertius*' type locality is also in the Nye Formation, Kimura and Barnes (2016) assign *Goedertius* to the early Miocene, likely on account of the specimen having been found further north, closer to the contact with the Astoria Formation.

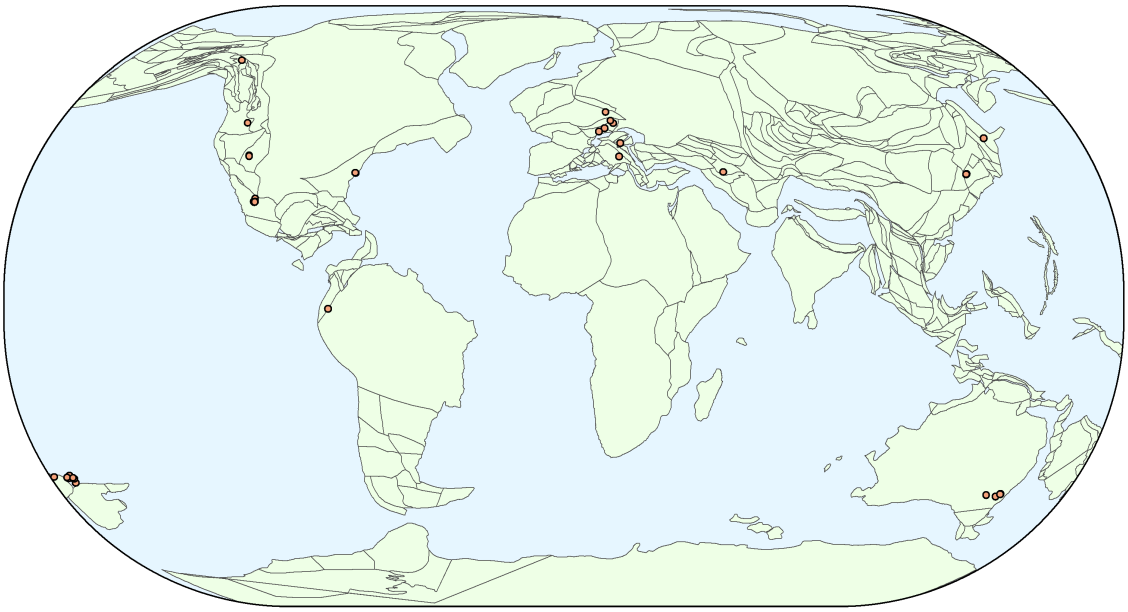

Figure 16 A map of the distribution of Platanistoidea during the Chattian (28-23 Ma). Data from the Paleobiology Database (PDBD); tectonic reconstructions created in Gplates. Note that the PBDB uses a more inclusive definition of the Platanistoidea, including the Squalodontidae.

The majority of platanistoids and other basal crown odontocetes are known from the early Miocene. *Chilcacetus* and *Huaridelphis* are tentatively dated to the early Miocene of Peru (Lambert et al., 2015). *Zarhachis flagellator*, a platanistid, existed from the early to middle Miocene of eastern North America (Cope, 1896; True, 1912); The platanistids *Araeodelphis* and *Dilophodelphis* are dated to the Burdigalian of eastern North America and Oregon, respectively (Boersma et al., 2017). *Zarhinocetus*, an allodelphinid, is from the early-middle Miocene of Washington state (Kimura and Barnes, 2016). Other basal crown odontocetes, such as the eurhinodelphinids *Eurhinodelphis* and *Xiphiacetus* are known from the early Miocene, though they may have appeared in the late Oligocene (Fordyce, 1983; Lambert, 2004). However, few of the odontocetes present in the early Miocene have been constrained to the Aquitanian, a

stage which is poorly known in the cetacean fossil record. There are the squalodelphinids *Squalodelphis* and *Notocetus* from Italy and Argentina, respectively, as well as a squalodelphinid from the Aquitanian Clallam Formation of the northeast Pacific (Nelson and Uhen, 2018); *Allodelphis woodburnei*, from the west coast of North America (Barnes and Reynolds, 2009), and *Zarhachis,* from the east coast of North America (Uhen, 2007). As mentioned earlier, *Goedertius*, dated to the Aquitanian, is also from the Nye Formation.

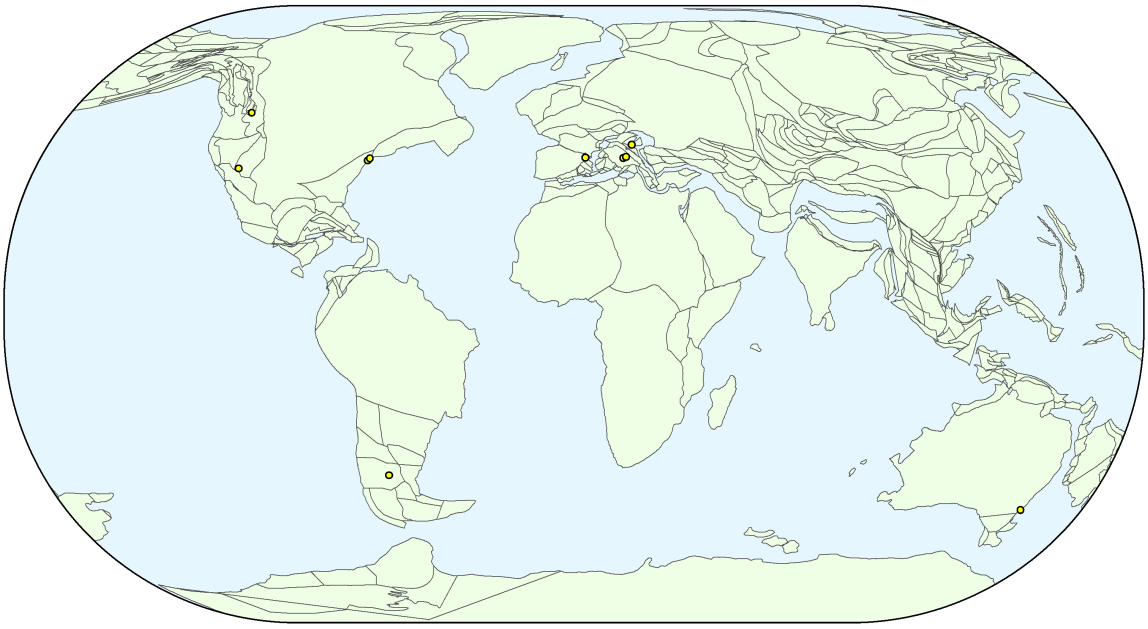

Figure 17 A map of the distribution of the Platanistoidea during the Aquitanian (23-20 Ma). Data from the Paleobiology Database (PDBD); tectonic reconstructions created in Gplates.

I argue under the Age and Stratigraphy section of the Systematic Paleontology that, given Lost Creek's proximity to the contact between the Nye Formation and the

underlying Yaquina Formation, *Perditicetus* was likely found in the lower Nye Formation and is plausibly Chattian in age. This would place *Perditicetus* as one of the earliest platanistoids, which is plausible given its basal position in phylogenetic analyses (Figure 18). Foraminiferal studies could confirm this; a Zemorrian fauna at the type locality would strongly suggest that *Perditicetus* is late Oligocene in age.

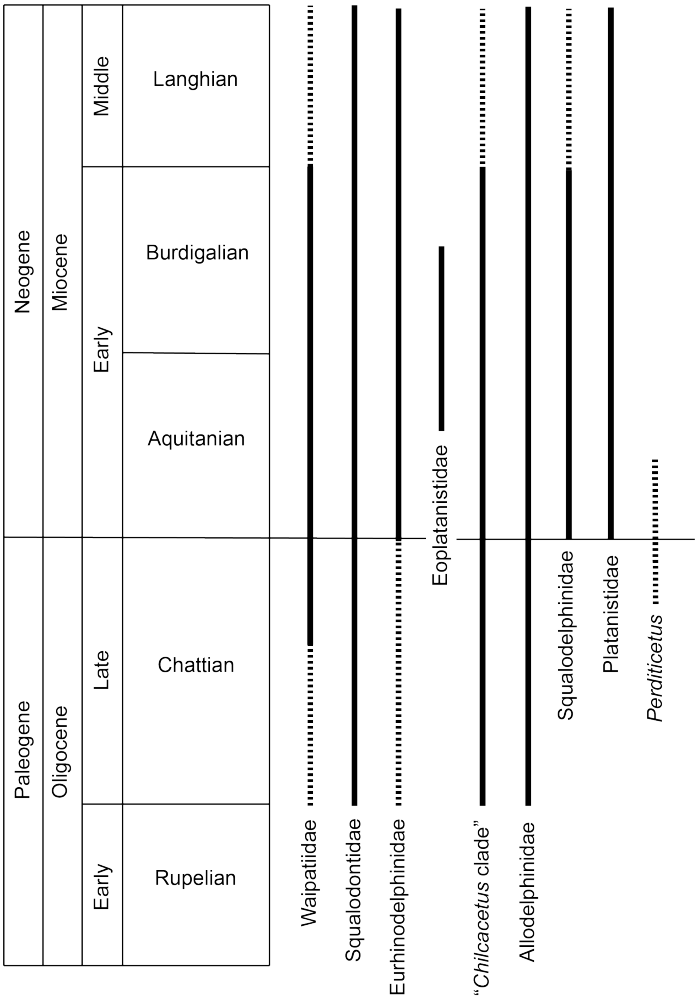

Figure 18 Range chart of the major groups of basal crown odontocetes discussed in this thesis. Stippled lines indicate range extensions based on tentatively identified or poorly dated material; or in the case of *Perditicetus*, on uncertainty of the type locality's position in the stratigraphy.

CONCLUSIONS

Perditicetus yaconensis displays a curious suite of characteristics: its skull resembles those of the basal crown odontocete *"Chilcacetus* clade", yet the morphology of the periotic allies *Perditicetus* firmly within the Platanistoidea. Further work with phylogenetic analyses is needed to more fully understand the possible relationship between the "*Chilcacetus* clade" and the Platanistoidea, as current phylogenies failed to capture similarity between the skull morphologies of odontocetes like *Chilcacetus*, and *Perditicetus*. The type locality south of Lost Creek appears to be closer to the lower contact between the Oligocene-Miocene boundary straddling Nye Formation and the underlying Yaquina Formation. If this is the case, then *Perditicetus* may well be one of the oldest platanistoids, especially if a definition excluding the Waipatiidae and Squalodontidae is considered.

APPENDIX

Codings for *Perditicetus yaconensis*, Analysis 1

010?? 01001 10140 ?101? ????? ????? ???10 ????? ??001 02010 02011 00010 11110 01000 00000 20?00 10000 01010 1000? 010?1 00112 11110 00001 010?? 00--1 310?1 00?00 00??? ???20 0??11 100?0 02?0? 0??10 11?20 ?010? 0?001 1001? 1?000 021?? ??0?? ??0?? ????? ????? ????? ????? ????? ????? ????? ????? ????? ????? ????? ????? ????? ????? ????? ????? ?? ?

Codings for *Perditicetus yaconensis*, Analysis 2

0?000 ?0001 00000 ?1?10 ?0??0 ????? 1???? ??001 00??? 00000 11002 ?1111 02001 0?

Codings for *Perditicetus yaconensis*, Analysis 3

0?000 00000 20001 00010 100-- -2020 1--10 00??1 ?0001 210?0 00000 ???0? ????? 1??0? ????? ??

REFERENCES

Addicott, W. O. 1976. Neogene molluscan stages of Oregon and Washington; pp. 95-115 in A. E. T. B. Fritsche, Harry Jr.; and Wornardt, W. W. (ed.), The Neogene symposium; selected technical papers on paleontology, sedimentology, petrology, tectonics and geologic history of the Pacific Coast of North America; tomorrow's oil from today's provinces.

Aguirre-Fernández, G., and R. E. Fordyce. 2014. *Papahu taitapu*, gen. et sp. nov., an early Miocene stem odontocete (Cetacea) from New Zealand. Journal of Vertebrate Paleontology 34:195-210.

Allen, G. M. 1921. A new fossil Cetacean. Bulletin of the Museum of Comparative Zoology 65:1–13.

Ameghino, F. 1891. Caracteres diagnósticos de cincuenta especies nuevas de mamiferos fósiles argentinos. Revista Argentina de Historia Natural 1:129–167.

Barnes, L. G. 1979. Fossil enaliarctine pinnipeds (Mammalia: Otariidae) from Pyramid Hill, Kern County, California. Contributions in Science, Natural History Museum of Los Angeles County 318:1–41.

Barnes, L. G. 2006. A phylogenetic analysis of the superfamily Platanistoidea (Mammalia, Cetacea, Odontoceti). Beiträge zur Paläontologie 30:25–42.

Barnes, L. G., and R. E. Reynolds. 2009. A new species of early Miocene allodelphinid dolphin (Cetacea, Odontoceti, Platanistoidea) from Cajon Pass, Southern California, U.S.A. Museum of Northern Arizona Bulletin 65:483–507.

Berta, A. 1991. New *Enaliarctos** (Pinnipedimorpha) from the Oligocene and Miocene of Oregon and the role of "enaliarctids" in pinniped phylogeny. Smithsonian Contributions to Paleobiology 69:1–33.

Berta, A. 1994. A new species of phocoid pinniped *Pinnarctidion* from the early Miocene of Oregon. Journal of Vertebrate Paleontology 14:405–413.

Bianucci, G., G. Bosio, E. Malinverno, C. de Muizon, I. M. Villa, M. Urbina, and O. Lambert. 2018. A new large squalodelphinid (Cetacea, Odontoceti) from Peru sheds light on the Early Miocene platanistoid disparity and ecology. Royal Society Open Science 5:172302.

Bianucci, G., M. Gatt, R. Catanzariti, S. Sorbi, C. G. Bonavia, R. Curmi, and A. Varola. 2011. Systematics, biostratigraphy and evolutionary pattern of the Oligo-Miocene marine mammals from the Maltese Islands. Geobios 44:549–585.

Bianucci, G., O. Lambert, R. Salas-Gismondi, J. Tejada, F. Pujos, M. Urbina, and P.-O. Antoine. 2013. A Miocene relative of the Ganges River dolphin (Odontoceti, Platanistidae) from the Amazonian Basin. Journal of Vertebrate Paleontology 33:741-745.

Bianucci, G., and W. Landini. 2002. A new short-rostrum odontocete (Mammalia: Cetacea) from the middle Miocene of the eastern Netherlands. Beaufortia 52:187–196.
Bianucci, G., M. Urbina, and O. Lambert. 2015. A new record of *Notocetus vanbenedeni* (Squalodelphinidae, Odontoceti, Cetacea) from the Early Miocene of Peru. Comptes Rendus Palevol 14:5-13.
Blainville, H. M. D., de. 1817. Delphinorhynques; pp. 151–152, Nouveau Dictionnaire d'Hisoire Naturelle. Deterville.
Boersma, A. T., M. R. McCurry, and N. D. Pyenson. 2017. A new fossil dolphin *Dilophodelphis fordycei* provides insight into the evolution of supraorbital crests in Platanistoidea (Mammalia, Cetacea). Royal Society Open Science 4:170022.
Boersma, A. T., and N. D. Pyenson. 2016. *Arktocara yakataga*, a new fossil odontocete (Mammalia, Cetacea) from the Oligocene of Alaska and the antiquity of Platanistoidea. PeerJ 4:e2321.
Bossley, M., A. Steiner, P. Brakes, J. Shrimpton, C. Foster, and L. Rendell. 2018. Tail walking in a bottlenose dolphin community: the rise and fall of an arbitrary cultural 'fad'. Biology Letters 14.
Burmeister, G. 1885. Exámen Crítico de los Mamíferos y Reptiles Fósiles denominados por D. Augusto Bravard. Anales del Museo Nacional de Buenos Aires:93–174.
Cabrera, Á. 1926. Cetáceos fósiles del Museo de La Plata. Revista del Museo de La Plata 29:363–411.
Cassens, I., S. Vicario, V. G. Waddell, H. Balchowsky, D. Van Belle, W. Ding, C. Fan, R. S. Lal Mohan, P. C. Simões-Lopes, R. Bastida, A. Meyer, M. J. Stanhope, and M. C. Milinkovitch. 2000. Independent adatpation to riverine habitats allowed survival of ancient cetacean lineages. Proceedings of the National Academy of Sciences of the United States of America 97:11343–11347.
Cope, E. D. 1868. Second contribution to the history of the Vertebrata of the Miocene period of the United States. Proceedings of the Academy of Natural Sciences of Philadelphia 20:184–194.
Cope, E. D. 1896. [Skull of a whale from the Miocene of the Yorktown epoch]. Science 3:880.
Costidis, A., and S. Rommel. 2012. Vascularization of Air Sinuses and Fat Bodies in the Head of the Bottlenose Dolphin (*Tursiops truncatus*): Morphological Implications on Physiology. Frontiers in Physiology 3.
Cozzuol, M. A. 1996. The record of the aquatic mammals in southern South America. Münchner Geowissenschaftliche Abhandlungen (A) 30:321–342.
Cranford, T. W., M. Amundin, and K. S. Norris. 1996. Functional morphology and homology in the odontocete nasal complex: implications for sound generation. Journal of Morphology 228:223–285.
Cranford, T. W., P. Krysl, and M. Amundin. 2010. A new acoustic portal into the odontocete ear and vibrational analysis of the tympanoperiotic complex. PLoS One 5:e11927.
Dal Piaz, G. 1908. Sui Vertebrati delle arenarie mioceniche di Belluno. Atti della Accademia Scientifica:106–120.

Dal Piaz, G. 1916. Gli Odontoceti del Miocene Bellunese, Parte Quarta: *Eoplatanista italica*. Memoirie dell'Instituto geologico della R. Università di Padova 5:1–25.
Dal Piaz, G. 1917. Gli Odontoceti del Miocene bellunese, Parte Terza. *Squalodelphis fabianni*. Memoirie dell'Instituto geologico della R. Università di Padova 5:1–34.
de Muizon, C. 1987. The affinities of *Notocetus vanbenedeni,* an Early Miocene platanistoid (Cetacea, Mammalia) from Patagonia, southern Argentina. American Museum Novitates 2904:1–27.
de Muizon, C. 1988. Le polyphylétisme des Acrodelphidae, Odontocètes longirostres du Miocène européen. Bulletin du Museum National d'Histoire Naturelle. Section C: Sciences de la Terre, Paleontologie, Geologie, Minerologie 10:31–88.
de Muizon, C. 1991. A new Ziphiidae (Cetacea) from the Early Miocene of Washington State (USA) and phylogenetic analysis of the major groups of odontocetes. Bulletin du Muséum National d'Histoire Naturelle, Paris 12:279–326.
de Muizon, C. 1994. Are the squalodonts related to the platanistoids? Proceedings of the San Diego Society of Natural History 29:135–146.
Domning, D. P. 2008. Desmostylia; pp. 639–644 in C. M. Janis, G. F. Gunnell, and M. D. Uhen (eds.), Evolution of Tertiary Mammals of North America. Cambridge University Press, Cambridge.
Domning, D. P., and C. E. Ray. 1986. The earliest sirenian (Mammalia: Dugongidae) from the eastern Pacific Ocean. Marine Mammal Science 2:263-276.
Dooley, A. C., Jr. 2005. A new species of *Squalodon* (Mammalia, Cetacea) from the Middle Miocene of Virginia. Virginia Museum of Natural History Memoirs 8:1–14.
Ekdale, E. G., and R. A. Racicot. 2015. Anatomical evidence for low frequency sensitivity in an archaeocete whale: comparison of the inner ear of *Zygorhiza kochii* with that of crown Mysticeti. Journal of Anatomy 226:22-39.
Fahlke, J. M., and O. Hampe. 2015. Cranial symmetry in baleen whales (Cetacea, Mysticeti) and the occurrence of cranial asymmetry throughout cetacean evolution. Naturwissenschaften 102:1309.
Fitzgerald, E. M. G. 2016. A late Oligocene waipatiid dolphin (Odontoceti: Waipatiidae) from Victoria, Australia. Memoirs of Museum Victoria 74:117-136.
Flynn, T. T. 1948. Description of *Prosqualodon davidi* Flynn, a fossil cetacean from Tasmania. Transactions of the Zoological Society of London 26:153–196.
Fordyce, R. E. 1983. Rhabdosteid dolphins (Mammalia: Cetacea) from the Middle Miocene, Lake Frome area, South Australia. Alcheringa 7:27–40.
Fordyce, R. E. 1994. *Waipatia maerewhenua*, new genus and new species (Waipatiidae, new family), an archaic Late Oligocene dolphin (Cetacea: Odontoceti: Platanistoidea) from New Zealand. Proceedings of the San Diego Society of Natural History 29:147–176.
Fordyce, R. E. 2002. *Simocetus rayi* (Odontoceti: Simocetidae, New Family): A bizarre new archaic Oligocene dolphin from the eastern North Pacific. Smithsonian Contributions to Paleobiology 93:185–222.
Fraser, F. C., and P. E. Purves. 1960. Hearing in cetaceans. Bulletin of the British Museum (Natural History) 7:1–140.

Geisler, J. H., M. W. Colbert, and J. L. Carew. 2014. A new fossil species supports an early origin for toothed whale echolocation. Nature 508:383-386.
Geisler, J. H., M. R. McGowen, G. Yang, and J. Gatesy. 2011. A supermatrix analysis of genomic, morphological, and paleontologial data from crown Cetacea. BMC Evolutionary Biology 11:1–33.
Gervais, P. 1861. Sur différentes espèces de vertébrés fossils observées pour la plupart dans le midi de la France. Mémoires de la Section des Sciences Académie des Sciences et Lettres de Montpellier 5:117–132.
Gervais, P., and A. d'Orbigny. 1844. Mammalogie. Société Philomatique de Paris. Extraits des Procès-verbaux des Séances 1844:38–40.
Godfrey, S. J., L. G. Barnes, and O. Lambert. 2017. The Early Miocene odontocete *Araeodelphis natator* Kellogg, 1957 (Cetacea; Platanistidae), from the Calvert Formation of Maryland, U.S.A. Journal of Vertebrate Paleontology:e1278607.
Goloboff, P. A. 1993. Estimating character weights during tree search. Cladistics 9:83-91.
Gonzalez-Barba, G. 2007. The Late Oligocene marine mammal assemblage of the San Juan and Timbabichi Members (El Cien Formation), Baja California Sur, Mexico. Geological Society of Australia Abstracts 85:43.
Gradstein, F. M., J. G. Ogg, and A. G. Smith. 2004. A Geologic Time Scale 2004. 589 pp. Cambridge University Press, Cambridge.
Grateloup, J. P. S. 1840. Catalogues des debris fossiles des corps organises decouverts dans les formations, geolgnostiques du bassin de la Gironde. Actes de l'Academie Nationale des Sciences, Belles-Lettres et Arts de Bordeaux 2:431–460, 693–716.
Guinet, C., and J. Bouvier. 1995. Development of intentional stranding hunting techniques in killer whale (*Orcinus orca*) calves at Crozet Archipelago. Canadian Journal of Zoology 73:27-33.
Hamilton, H., S. Caballero, A. G. Collins, and R. L. Brownell, Jr. 2001. Evolution of river dolphins. Proceedings of the Royal Society of London Series B: Biological Sciences:549–556.
Hulbert, R. C., Jr. , and F. C. Whitmore. 2006. Late Miocene mammals for the Mauvilla Local Fauna, Alabama. Bulletin of the Florida Museum of Natural History 46:1–28.
Hulbert, R. C., Jr., R. M. Petkewich, G. A. Bishop, D. Bukry, and D. P. Aleshire. 1998. A new middle Eocene protocetid whale (Mammalia: Cetacea: Archaeoceti) and associated biota from Georgia. Journal of Paleontology 72:907–927.
Huxley, T. H. 1859. On a fossil bird and a fossil cetacean from New Zealand. Quarterly Journal of the Geological Society of London 15:670–677.
Kellogg, R. 1957. Two additional Miocene porpoises from the Calvert Cliffs Maryland. Proceedings of the United States National Museum 107:279–337.
Kimura, T., and L. G. Barnes. 2016. New Miocene fossil Allodelphinidae (Cetacea, Odontoceti, Platanistoidea) from the North Pacific Ocean. Bulletin of the Gunma Museum of Natural History 20:1-58.
Lambert, O. 2004. Systematic revision of the Miocene long-snouted dolphin *Eurhinodelphis longirostris* Du Bus, 1872 (Cetacea, Odontoceti,

Eurhinodelphinidae). Bulletin de l'Institut Royal des Sciences Naturelles de Belgique: Sciences de la Terre 74:147–174.
Lambert, O. 2005a. Phylogenetic affinities of the long-snouted dolphin *Eurhinodelphis* (Cetacea, Odontoceti) from the Micoene of Antwerp, Belgium. Palaeontology 48:653–679.
Lambert, O. 2005b. Review of the Miocene long-snouted dolphin *Priscodelphinus cristatus* du Bus, 1872 (Cetacea, Odontoceti) and phylogeny among eurhinodelphinids. Bulletin de l'Institut Royal des Sciences Naturelles de Belgique: Sciences de la Terre 75:211–235.
Lambert, O., G. Bianucci, and M. Urbina. 2014. *Huaridelphis raimondii*, a new early Miocene Squalodelphinidae (Cetacea, Odontoceti) from the Chilcatay Formation, Peru. Journal of Vertebrate Paleontology 34:987-1004.
Lambert, O., C. de Muizon, and G. Bianucci. 2015. A new archaic homodont toothed cetacean (Mammalia, Cetacea, Odontoceti) from the early Miocene of Peru. Geodiversitas 37:79-108.
Lambert, O., C. de Muizon, E. Malinverno, C. D. Celma, M. Urbina, and G. Bianucci. 2017. A new odontocete (toothed cetacean) from the Early Miocene of Peru expands the morphological disparity of extinct heterodont dolphins. Journal of Systematic Palaeontology:1-36.
Lambert, O., S. J. Godfrey, and E. M. G. Fitzgerald. 2019. *Yaquinacetus meadi*, a new latest Oligocene–early Miocene dolphin (Cetacea, Odontoceti, Squaloziphiidae, fam. nov.) from the Nye Mudstone (Oregon, U.S.A.). Journal of Vertebrate Paleontology:e1559174.
Lambert, O., and S. Louwye. 2006. *Archaeoziphius microglenoideus*, a new primitive beaked whale (Mammalia, Cetacea, Odontoceti) from the middle Miocene of Belgium. Journal of Vertebrate Paleontology 26:182–191.
Lebeck, H. J. 1801. *Delphinus gangeticus* beschrieben von Heinrich Julius Lebeck zu Trankenbar. Der Gesellschaft naturforschender Freude zu Berlin Neue Schriften 3.
Lee, Y.-N., H. Ichishima, and D. K. Choi. 2012. First record of a platanistoid cetacean from the middle Miocene of South Korea. Journal of Vertebrate Paleontology 32:231–234.
Leidy, J. 1869. The extinct mammalian fauna of Dakota and Nebraska, including an account of some allied forms from other localities, together with a synopsis of the mammalian remains of North America. Journal of the Academy of Natural Sciences of Philadelphia 2:1–472.
Leidy, J. 1877. Description of vertebrate remains, chiefly from the phosphate beds of South Carolina. Journal of the Academy of Natural Sciences of Philadelphia 8:209–261.
Loch, C., and P. C. Simoes-Lopes. 2013. Dental wear in dolphins (Cetacea: Delphinidae) from southern Brazil. Archives of Oral Biology 58:134-141.
Luo, Z., and P. D. Gingerich. 1999. Terrestrial Mesonychia to aquatic Cetacea: Transformation of the basicranium and evolution of hearing in whales. University of Michigan Papers on Paleontology 31:1–98.

Lydekker, R. 1892. On zeuglodont and other Cetacean remains from the Tertiary of the Causcasus. Proceedings of the Zoological Society of London 1893:558–564.
Lydekker, R. 1893. Cetacean skulls from Patagonia. Annales del Museo de la Plata Paleontología Argentina II:1–13.
Marino, L., R. C. Connor, R. E. Fordyce, L. M. Herman, P. R. Hoff, L. Lefebvre, D. Lusseau, B. McCowan, E. A. Nimchinsky, A. A. Pack, L. Rendell, J. S. Reidenberg, D. Reiss, M. D. Uhen, E. Van der Gucht, and H. Whitehead. 2007. Cetaceans have complex brains for complex cognition. PLoS Biology 5:966–972.
Marsh, O. C. 1888. Notice of a new fossil Sirenian, from California. The American Journal of Science 35:94–96.
Marx, F. G., O. Lambert, and M. D. Uhen. 2016. Cetacean Paleobiology. 319 pp. Wiley Blackwell, Oxford.
McCurry, M. R., and N. D. Pyenson. 2018. Hyper-longirostry and kinematic disparity in extinct toothed whales. Paleobiology.
McGowen, M. R., M. Spaulding, and J. Gatesy. 2009. Divergence date estimation and a comprehensive molecular tree of extant cetaceans. Molecular Phylogenetics and Evolution 53:891–906.
Mchedlidze, G. A. 1976. Osnovnye Cherty Paleobiologischeskoi Istorii Kitoobraznykh. 136 pp. Metsnierba Publishers, Tbilisi, Georgia.
McKeel, D. R., and J. H. Lipps. 1972. Calcareous plankton from the Tertiary of Oregon. Palaeogeography, Palaeoclimatology, Palaeoecology 12:75-93.
McKenna, M. F., T. W. Cranford, A. Berta, and N. D. Pyenson. 2012. Morphology of the odontocete melon and its implications for acoustic function. Marine Mammal Science 28:690-713.
Mead, J. G., and R. L. Brownell. 2005. Order Cetacea; pp. 723–743 *i*n D. E. Wilson, and D. M. Reeder (eds.), Mammal Species of the World. The Johns Hopkins University Press, Baltimore.
Mead, J. G., and R. E. Fordyce. 2009. The therian skull: A lexicon with emphasis on the odontocetes. Smithsonian Contributions to Zoology 627:1–248.
Miller, G. S., Jr. 1918. A new river-dolphin from China. Smithsonian Miscellaneous Collections 68:1–12.
Mitchell, E. D., and R. H. Tedford. 1973. The Enaliarctinae: A new group of extinct aquatic carnivora and a consideration of the origin of the Otariidae. Bulletin of the American Museum of Natural History 151:203–284.
Moreno, F. P. 1892. Lijeros apuntes sobre dos géneros de cetáceos fósiles de la República Argentina. Revista del Museo de La Plata 3:393–400.
Nelson, M. D., and M. D. Uhen. 2018. First occurrence of a squalodelphinid (Cetacea, Odontoceti) from the early Miocene of Washington State. Journal of Vertebrate Paleontology 38.
Nesbitt, E. A. 2018. Cenozoic Marine Formations of Washington and Oregon: an annotated catalogue. PaleoBios 35:1-20.
Prothero, D. R., C. Z. Bitboul, G. W. Moore, and A. R. Niem. 2001. Magnetic stratigraphy and tectonic rotation of the Oligocene Alsea, Yaquina, and Nye Formations, Lincoln County, Oregon; pp. 184–194 in D. R. Prothero (ed.),

Magnetic Stratigraphy of the Pacific Coast Cenozoic. The Pacific Section SEPM, Sante Fe Springs, CA.
Pyenson, N., and S. N. Sponberg. 2011. Reconstructing body size in extinct crown Cetacea (Neoceti) using allometry, phylogenetic methods and tests from the fossil record. Journal of Mammalian Evolution 18:269–288.
Pyenson, N. D., J. Velez-Juarbe, C. S. Gutstein, H. Little, D. Vigil, and A. O'Dea. 2015. *Isthminia panamensis*, a new fossil inioid (Mammalia, Cetacea) from the Chagres Formation of Panama and the evolution of 'river dolphins' in the Americas. PeerJ 3:e1227.
Rothausen, K. 1968. Die systematisch Stellung der europäischen Squalodontidae (Odontoceti, Mamm.). Paläontologische Zeitschrift 42:83–104.
Sanders, A. E., and J. H. Geisler. 2015. A new basal odontocete from the upper Rupelian of South Carolina, U.S.A., with contributions to the systematics of *Xenorophus* and *Mirocetus* (Mammalia, Cetacea). Journal of Vertebrate Paleontology 35:e890107.
Schenck, H. G. 1927. Marine Oligocene of Oregon. University of California Publication in Geological Sciences 16:449-460.
Schorr, G. S., E. A. Falcone, D. J. Moretti, and R. D. Andrews. 2014. First long-term behavioral records from Cuvier's beaked whales (*Ziphius cavirostris*) reveal record-breaking dives. PLoS One 9:e92633.
Simpson, G. G. 1945. The principles of classification and a classification of mammals. Bulletin of the American Museum of Natural History 85:1–350.
Smith, W. D. 1926. Physical and economic geography of Oregon; the Coast Range province. The Commonwealth Review of the University of Oregon 8:254-297.
Snavely, P. D., Jr.; , W. W. Rau, and H. C. Wagner. 1964. Miocene stratigraphy of the Yaquina Bay area, Newport, Oregon. The Ore Bin 26:133-152.
Spoor, F., S. Bajpai, S. T. Hussain, K. Kumar, and J. G. M. Thewissen. 2002. Vestibular evidence for the evolution of aquatic behavior in early cetaceans. Nature 417:163–166.
Stirton, R. A. 1960. A marine carnivore from the Clallam Miocene Formation Washington. University of California Publications in Geological Sciences 36:345-368.
Swofford, D. L. 2002. PAUP* Phylogenetic Analysis Using Parsimony (* and Other Methods). Sinauer Associates, Sunderland, Massachusetts.
Tanaka, Y., J. Abella, G. Aguirre-Fernandez, M. Gregori, and R. E. Fordyce. 2017. A new tropical Oligocene dolphin from Montanita/Olon, Santa Elena, Ecuador. PLoS One 12:e0188380.
Tanaka, Y., and R. E. Fordyce. 2014. Fossil dolphin *Otekaikea marplesi* (Latest Oligocene, New Zealand) expands the morphological and taxonomic diversity of Oligocene cetaceans. PLoS One 9:e107972.
Tanaka, Y., and R. E. Fordyce. 2015a. Historically significant late Oligocene dolphin *Microcetus hectori* Benham 1935: a new species of *Waipatia* (Platanistoidea). Journal of the Royal Society of New Zealand:1-16.

Tanaka, Y., and R. E. Fordyce. 2015b. A new Oligo-Miocene dolphin from New Zealand: Otekaikea huata expands diversity of the early Platanistoidea. Palaeontologia Electronica 18:1-71.
Tanaka, Y., and R. E. Fordyce. 2017. *Awamokoa tokarahi*, a new basal dolphin in the Platanistoidea (late Oligocene, New Zealand). Journal of Systematic Palaeontology 15:365-386.
Tedford, R. H., L. G. Barnes, and C. E. Ray. 1994. The early Miocene littoral ursoid carnivoran *Kolponomos*: Systematics and mode of life. Proceedings of the San Diego Society of Natural History 29:11–32.
True, F. W. 1908. The fossil cetacean, *Dorudon serratus* Gibbes. Bulletin of the Museum of Comparative Zoology 52:65–78.
True, F. W. 1912. Description of a new fossil porpoise of the genus *Delphinodon* from the Miocene Formation of Maryland. Journal of the Academy of Natural Sciences of Philadelphia 15:165–193.
Uhen, M. D. 2007. USNM Chesapeake Group Cetacean Collection Data.
Van Beneden, P. J., and P. Gervais. 1880. Ostéographie des Cétacés Vivants et Fossiles. 634 pp. Arthus Bertrand, Paris.
Vokes, H. E., H. Norbisrath, and P. D. Snavely, Jr. 1949. Geology of the Newport-Waldport area, Lincoln and Lane Counties, Oregon: In *U.S. Geological Survey Oil and Gas Investigations Preliminary Map*. United States Geological Survey.
Werth, A. J. 2000. Feeing in marine mammals; pp. 487-526, Feeding: Form, Function and Evolution in Tetrapod Vertebrates. Academic Press, San Diego.
Wilson, L. E. 1935. Miocene marine mammals from the Bakersfield region, California. The Peabody Museum of Natural History Bulletin 4:1–143.

BIOGRAPHY

Margot D. Nelson graduated from Forest Ridge School of the Sacred Heart, Bellevue, Washington, in 2010. She received her Bachelor of Science in Earth and Space Sciences and Biology from University of Washington, in Seattle, in 2015. Margot has been a Graduate Teacher's Assistant, teaching the introductory geology labs at George Mason University. She has been accepted into George Mason University's PhD program in Environmental Science and Policy; she plans to continue studying fossil whales with her advisor, Dr. Mark D. Uhen. In her leisure time, Margot enjoys the company of her horses and studies classical piano.